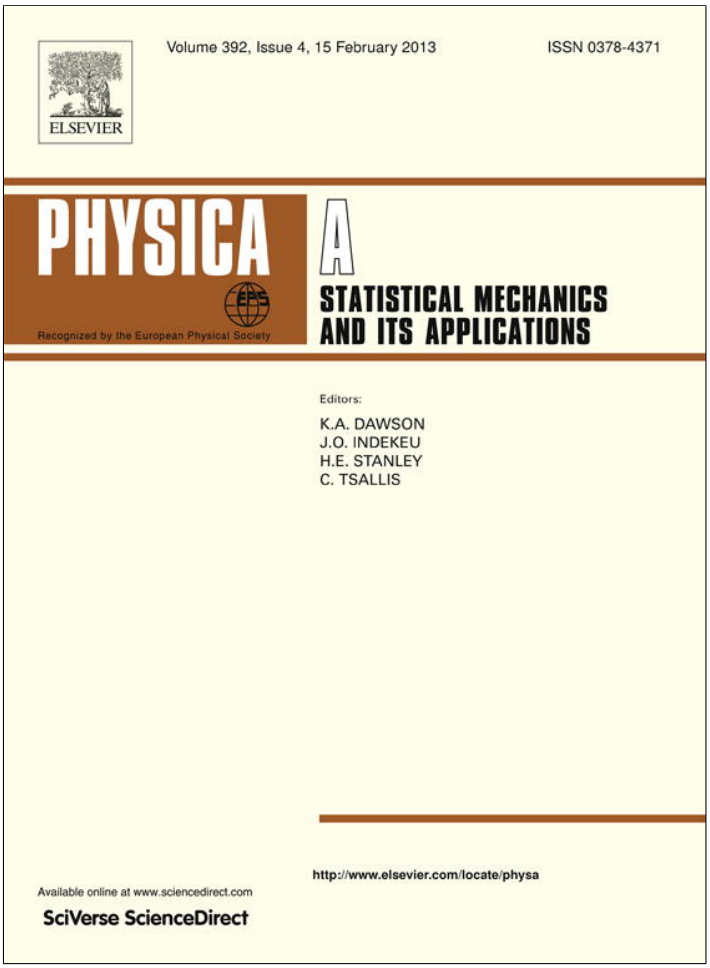

Physica A 392 (2013) 1004–1027

Contents lists available at SciVerse ScienceDirect

Physica A

journal homepage: www.elsevier.com/locate/physa

The origin of power-law emergent scaling in large binary networks

D.P. Almond, C.J. Budd, M.A. Freitag, G.W. Hunt, N.J. McCullen *, N.D. Smith

Center for Nonlinear Mechanics, University of Bath, BA2 7AY, UK

ARTICLE INFO

Article history:
Received 25 April 2012
Received in revised form 3 September 2012
Available online 2 November 2012

Keywords:
Emergent scaling
Complex systems
Binary networks
Composite materials
Effective medium approximation
Dielectric response
Generalised eigenvalue spectrum

ABSTRACT

We study the macroscopic conduction properties of large but finite binary networks with conducting bonds. By taking a combination of a spectral and an averaging based approach we derive asymptotic formulae for the conduction in terms of the component proportions p and the total number of components N. These formulae correctly identify both the percolation limits and also the emergent power-law behaviour between the percolation limits and show the interplay between the size of the network and the deviation of the proportion from the critical value of $p = 1/2$. The results compare excellently with a large number of numerical simulations.

1. Introduction and summary

Large but finite binary networks comprising disordered mixtures of two interacting components can arise both directly, in electrical circuits [1–4] or mechanical structures [5], and as models of other systems such as disordered materials with varying electrical [6], thermal, mechanical or even geophysical properties in the micro-scale, coupled at a meso-scale [7]. They are prototypes of many forms of *complex systems* which are often observed to have *macroscopic emergent properties* which can have *emergent power-law behaviour* over a wide range of parameter values which is different from any power-law behaviour of the individual elements of the network, and is a consequence of the way in which the responses of the components *combine*. For certain ranges of parameters we see the extensively studied *percolation type* of behaviour [8], in which the overall conductance is directly proportional to the individual component conductances with a constant of proportionality dependent both on the component proportion and on the network size. In this paper, we will combine a spectral analysis, motivated by Jonckheere and Luck [9], of the (partly random) linear operators (Kirchhoff-type matrices) associated with the network, with the averaging methods described in Ref. [4], to derive a universal asymptotic formula for the emergent network admittance, that includes both the effects of the *component proportion p* and the *network size N*.

We consider (a set of random realisations of) a binary square network comprising a random mixture of N *conducting bonds* which are either chosen to have a constant admittance y_1 or a variable admittance y_2. If p is the occupation probability for choosing a y_2 component, and $(1 - p)$ the occupation probability for y_1, in the limit of large N or for averages over large numbers of systems, it directly determines the proportion of y_2 to be approximately p and y_1 to be $(1 - p)$. We set the admittance ratio to be

$$\mu = y_2/y_1$$

and will assume that μ is an experimentally variable parameter. In particular we will assume that $y_1 = 1/R$ is resistive (real) and that y_2 is either resistive, in which case μ is real and positive, or y_2 is reactive (for example $y_2 = \mathrm{i}\omega C$ where C

* Corresponding author.
E-mail address: n.mccullen@physics.org (N.J. McCullen).

0378-4371/$ – see front matter © 2012 Elsevier B.V. All rights reserved.
doi:10.1016/j.physa.2012.10.035

is a capacitance and ω is a variable applied angular frequency), so that μ is pure imaginary. If μ is varied then the system has a total admittance $Y(\mu)$ which emerges from the combination of the admittance pathways through the various bonds in the network. Over a wide range of values $0 < \mu_1 < |\mu| < \mu_2$, both types of bond can be considered to conduct and the admittance displays a combined *power-law emergent characteristic* so that $Y(\mu)$ is proportional to $y_1^{1-\alpha}y_2^{\alpha}$ with an exponent $\alpha(p) \approx p$. The effects of network size, and component proportion, are important in that μ_1 and μ_2 depend upon both p and N, and it is well known [8] that the case $p = 1/2$ is a *critical value* (p_c) for two-dimensional square networks. If $p \neq 1/2$ and N is sufficiently large then this problem can be studied by the averaging and the *effective medium approximation, EMA* described in Ref. [4], with $\mu_1 \to 0$ and $\mu_2 \to \infty$ as $p \to 1/2$. This approximation breaks down if $p \approx 1/2$ and N is not very large. When $p = 1/2$, then in the power-law range $\mu_1 < |\mu| < \mu_2$ we have the well known duality result $Y = \sqrt{y_1 y_2}$ [10] and we will show in this paper that μ_1 is inversely proportional to N and μ_2 directly proportional to N, for large N. In contrast to the power-law behaviour, when either $0 < |\mu| < \mu_1$ or $|\mu| > \mu_2$ *percolation type* behaviour is observed, in which the conducting bonds are either those with conductance y_1 or y_2 respectively. In this case, if $p < 1/2$ then in all realisations of the network, Y is proportional to y_1, and if $p > 1/2$, Y is proportional to y_2, with constants of proportionality dependent on $|p - 1/2|$. If $p = 1/2$, half of the realisations have Y proportional to y_1 and the other half to y_2. Hence we see in this system (i) an emergent region with a power-law response depending on the proportion but not the arrangement or number of the components, (ii) a more random region and (iii) a transition between these two regions at frequency values which depends on the number and proportion of components in the system. Illustrations of the different types of observed response will be shown in Section 2.

The purpose of this paper is to give insight into both the emergent power law and percolation behaviour by obtaining asymptotic formulae for the expected response curves. To do this we extend and combine results obtained by two complementary methods, one based upon averaging [4] and the other based on properties of the spectrum of certain operators [9]. The averaging method works well when $p \neq 1/2$ and $N \to \infty$, and the spectral method, in contrast, works well for the case of $p = 1/2$ and large, finite N. The spectral method is based both on rigorous results concerning the poles and zero distribution of the function $Y(\omega)$ and on certain semi-empirical results on the regularity of their statistical distribution.

To describe these results we set $\epsilon = p - 1/2$ to measure the deviation from criticality, and set $\theta = Y/\sqrt{y_1 y_2}$. In Section 6 we will then combine the spectral and averaging methods to derive asymptotic formulae valid over a range of values for which ϵ is small and N is large. In particular, if $\epsilon > 0$

$$\theta - \frac{1}{\theta} + \epsilon\left(\sqrt{\mu} - \frac{1}{\sqrt{\mu}}\right) = \frac{1}{N}\left(\frac{1}{\mu\theta} - \mu\theta\right) \tag{1}$$

and if $\epsilon < 0$ then

$$\theta - \frac{1}{\theta} + \epsilon\left(\sqrt{\mu} - \frac{1}{\sqrt{\mu}}\right) = \frac{1}{N}\left(\frac{\mu}{\theta} - \frac{\theta}{\mu}\right), \tag{2}$$

with two further formulae (35) and (36) corresponding to the two other different percolation behaviours which arise when $\epsilon = 0$. We can see a variety of different behaviours summarised in these expressions (and derived in Section 6). If $N = \infty$ (so that $1/N = 0$), then these expressions reduce to the EMA results [4] and they predict that there is power-law behaviour if $\mu_1 < |\mu| < \mu_2$. If $\epsilon > 0$ we have $\mu_1 = 1/\mu_2 = \epsilon^{1/p}$ and for large $|\mu|$, $Y = y_1/\epsilon$. If $\epsilon < 0$ then $\mu_1 = 1/\mu_2 = (-\epsilon)^{1/(1-p)}$ and for large $|\mu|$, $Y = -\epsilon y_2$. (We note that the EMA prediction is not particularly good in the limit of $p \to 1/2$. In particular, it has been observed empirically [9] that rather than having percolation limits proportional to $|1/2 - p|$ or $|1/2 - p|^{-1}$, in the limit of $|1/2 - p| \ll 1$ they are more closely approximated by expressions of the form $|Y| \sim |1/2 - p|^{\pm\beta}$, $\beta \approx 1.3$.)

In contrast, if $\epsilon = 0$ and $1 \ll N < \infty$ then we show in Section 5 that

$$\mu_1 = 1/N, \qquad \mu_2 = N \tag{3}$$

and for large $|\mu|$ we may observe limits of either

$$Y = y_2/\sqrt{N}, \quad \text{or} \quad Y = \sqrt{N}y_1 \tag{4}$$

depending upon the percolation path taken.

Perhaps the most interesting behaviour is found when neither ϵ nor $1/N$ equal zero (but are both close to zero). In this case the expressions (1) and (2) predict that when $N \gg 1/\epsilon^2$ we see behaviour of the form described by the EMA approximation, whereas if ϵ is small and $1 \ll N \ll 1/\epsilon^2$ the behaviour is closer given when $\epsilon = 0$, summarised in (3) and (4). This transition is illustrated in Fig. 6 in Section 2.

The layout of the remainder of this paper is as follows. In Section 2 we will give a series of numerical results for a general binary network with admittances y_1 and y_2, looking at both power-law emergent behaviour and at percolation responses. These will illustrate the various points made above on the nature of the network response and give numerical evidence for the asymptotic formulae (1) and (2). In Section 3 we will formulate the matrix equations describing the network and derive the admittance function. In Section 4 we will discuss, and derive, a series of statistical results concerning the distribution of the poles and zeros of this function. In Section 5 we will use these statistical results to derive a precise asymptotic form of the admittance Y of a general binary network, when $p = 1/2$ and N is large. In Section 6 we review the (classical) averaging method for $N = \infty$ which gives an excellent estimate when p is not too close to $1/2$, and will also consider a combination

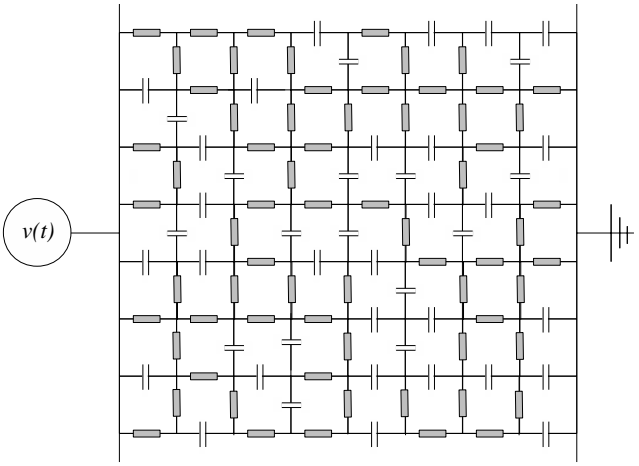

Fig. 1. Illustration of an example resistor capacitor circuit.

of this method with the spectral method for finite N, leading to the formulae (59) and (60) for the response for all p and sufficiently large N. In Section 7 we compare the predictions of the asymptotic formulae with numerical computations of the network responses. Finally in Section 8 we will draw some conclusions from this work.

2. Network models and their responses

This section will detail the various basic models for composite materials and associated random binary electrical networks described in the introduction. We will present the graphs of their responses, comparing power law and percolation type responses, and will provide evidence for the asymptotic behaviours for these described in the formulae (1) and (2).

2.1. Composite materials and their properties

A motivation for studying binary networks comes from models of disordered two-phase composite materials which are found to exhibit power-law scaling in their bulk responses over several orders of magnitude in the contrast ratio of the components [11,2,1,12]. In the electrical experiments this was previously referred to as "Universal Dielectric Response" (UDR), and it has been observed [13,14] that this is an emergent property arising out of the random nature of the mixture. For a binary disordered mixture, the different components can then be assigned randomly to the bonds on the lattice [15] and in most previous studies a 2D square lattice has been used, with the admittance of the bonds assigned randomly as either $y_2 = \mathrm{i}\omega C$ or $y_1 = 1/R$, with probability p, $1-p$ respectively and for which $\mu = \mathrm{i}\omega CR$. For convenience we consider this case in this section, and the more general case later in the paper. The components are distributed in a two-dimensional lattice between two bus-bars, one of which is grounded and the other is raised to a potential $V(t)$. Such a network is illustrated in 1. The network will have a current $I(t)$ between the bus-bars, and the macroscopic (complex) admittance is given by

$$Y = I/V.$$

There are many advantages to using network representations of these types of systems. In particular, widely available circuit simulation software can be used, which makes use of the available efficient sparse-matrix techniques in solving the equations of the system, allowing many different simulations to be made of different realisations of the circuit with randomly assigned resistors and capacitors. These techniques were used in various studies to show that the power-law behaviour exists in any binary random network over a range of values of the contrast ratio μ [15,16,3,5,17]. Furthermore, finite element calculations reported in Ref. [17] indicate that the response of the full material is very close to that of the network model of that material. These studies complement those of percolation in such binary disordered networks over limiting values of μ described, for example, in Refs. [9,2,8].

2.2. Percolation and power-law emergent behaviour

We describe the qualitative form of the conducting behaviour of these networks as ω varies. When $|\mu| = \omega CR \ll 1$, the capacitors act as open circuits and conduction occurs predominantly through the resistors. The circuit then becomes a *percolation network* in which the bonds are either conducting with probability $(1-p)$ or non-conducting with probability p. The network then only conducts macroscopically if there is a percolation path from one electrode to the other. It is well known [18] that, for 2D square lattices, there is a *critical percolation probability*,

$$p_c = 1/2,$$

and if $p < p_c$ then such a path exists with probability approaching one as the network size increases, and is resistive, so that the overall admittance is independent of ω. If $p > p_c$ then there is a very low probability of a resistive conduction path, and

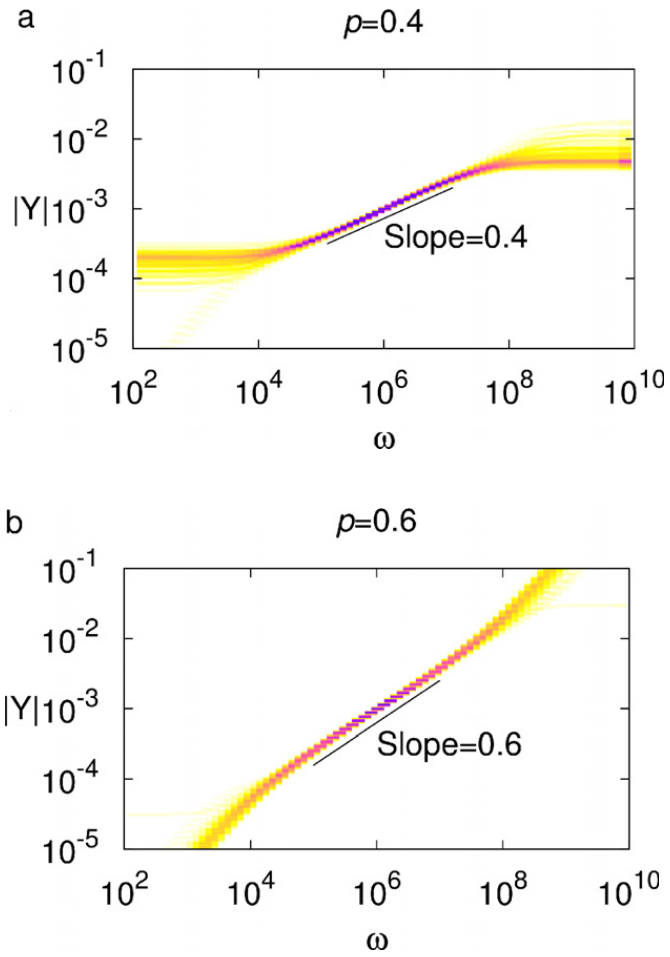

Fig. 2. (Color online) Typical responses of network simulations for values of $p \neq 1/2$ which give qualitatively different behaviour so that in the percolation region with $\omega \ll (CR)^{-1} = 10^6 s^{-1}$ or $\omega \gg (CR)^{-1}$, we see resistive behaviour in case (a) and capacitative behaviour in case (b). The figures presented are density plots of 100 random realisations for a 20×20 network. Note that all of the realisations give very similar results.

all paths between the electrodes will contain reactive elements, with the resulting overall admittance being proportional to ω. The case of $p = p_c = 1/2$ is critical, with a 50% probability that a resistive conducting path exists. Half of the realisations of the network will give an admittance response independent of ω and half an admittance response proportional to ω. When $|\mu| = \omega CR \gg 1$, we see an opposite response. In this case the capacitors act as almost short circuits with far higher admittance than the resistors which act as open circuits. Thus, if $p > p_c$ we see a response proportional to ω and if $p < p_c$ a response independent of ω. The case of $p = p_c$ again leads to both types of response having equal likelihood of occurrence, depending upon the network configuration. Note that this implies that if $p = 1/2$ then there are *four possible qualitatively different* types of percolation response for any random realisation of the system. For *intermediate values* of ω the values of the admittance of the resistors and the capacitors are much closer to each other and it is here that we see emergent power-law emergent behaviour. This is characterised by an admittance response $|Y|$ that is proportional to ω^α, $\alpha \approx p$ over a range $\omega \in (\omega_1, \omega_2)$ and which *is not randomly dependent upon the network configuration*. In Fig. 2(a) and (b) we plot the admittance response for many different realisations of a network in which $C = 1$ nF, and $R = 1$ kΩ, as a function of ω in the cases of $p = 0.4 < p_c$, $p = 0.6 > p_c$ and in Fig. 3 for $p = p_c = 1/2$. These figures clearly demonstrate the forms of behaviour described above and in the Introduction. Observe that in all cases we see quite a sharp transition between the percolation type behaviour and the power-law emergent behaviour as ω varies, that in all cases the exponent of the power law is close to p.

We have seen above how the response of the network depends strongly upon p. It also depends upon the network size N, and this effect is especially significant if $p = p_c = 1/2$. In Fig. 4 we fix $p = p_c$ and show how the form of $|Y|$ depends on N. Observe that in this case the width of the power-law emergent region increases apparently without bound, as N increases, as do the magnitude of the responses for small and large frequencies. From these graphs, it is apparent that in this critical case the upper limit of the power-law emergent region is proportional to N and the lower limit proportional to $1/N$. This is consistent with the formulae (3) and (4), presented in the Introduction. We can roughly motivate the result for $p = 1/2$ as follows. Suppose that ω is small so that the capacitors essentially act as open circuits. Imagine for a single percolation path through all of these capacitors comprising a chain of resistors, then this will have an approximate length of $\sqrt{N}$ resistors and hence a conductance of $1/(\sqrt{N}R)$. In contrast, if there is a dual path of capacitors going from top to bottom of the network, interrupting the resistors, then each resistive path has conductance $i\omega C$ and there are $\sqrt{N}$ of these in parallel, so that the

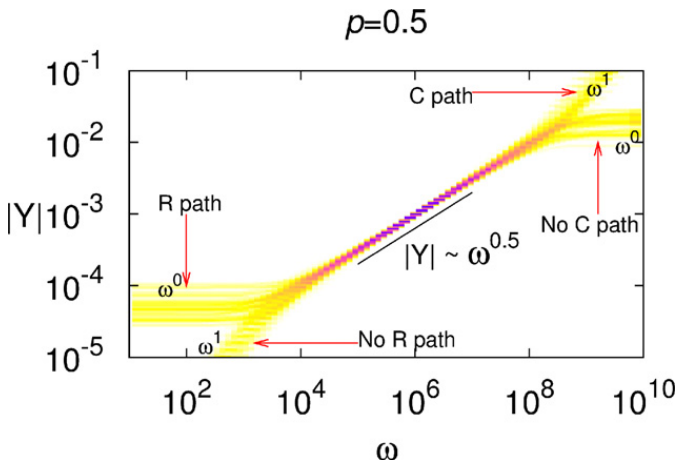

Fig. 3. (Color online) Responses for 100 realisations at $p = 1/2$ showing four different qualitative types of response for different realisations. Here, about half of the responses have a resistive percolation path and half have a capacitive one at low frequencies, with a similar behaviour at high frequencies. The responses at high and low ω indicate which of these cases exist for a particular realisation. The power-law emergent region can also be seen in which the admittance scales as $\sqrt{\omega}$ and all of the responses of the different network realisations coincide.

overall conductance is $\sqrt{N}i\omega C$. In Fig. 5 we plot the response for $p = 0.4$ and again increase N. In contrast to the former case, away from $p = 1/2$, the size of the power-law emergent region appears to scale with N for small N before becoming asymptotic to a finite value for larger values of N.

2.3. The effects of network size and bond proportions

To compare these results and to investigate the interplay between network size and the proportion p, we consider for $p \leq p_c$ the response for those realisations which have a resistive percolation path for both low and high frequencies. We define the *dynamic range* $\hat{Y}(N, p)$ by

$$\hat{Y} = \frac{|Y|_{\max}}{|Y|_{\min}} = \frac{|Y|(\omega \to \infty)}{|Y|(\omega \to 0)}.$$

In Fig. 6(a) we plot $\hat{Y}$ as a function of N for a variety of values of $p \leq 1/2$. We see from this figure that if $p = 1/2$ then $\hat{Y}$ is directly proportional to N for all values of N. In contrast, if $p < 1/2$ then $\hat{Y}$ is directly proportional to N for smaller values of N and then becomes asymptotic to a finite value $\hat{Y}(p)$ as $N \to \infty$. The transition between these two forms of behaviour occurs when $N > (1/2 - p)^{-2}$. This behaviour can be understood in terms of the asymptotic formulae (1) and (2) given in the Introduction. We will show in Section 5 that these imply that $\hat{Y}$ is approximated by β^2 where β satisfies the quadratic equation

$$\frac{\beta^2}{N} + (1 - 2p)\beta - 1 = 0. \tag{5}$$

The expression (5) gives reasonable qualitative agreement with the calculations presented in Fig. 6 with $\hat{Y} \sim N$ for smaller values of N and $\hat{Y} \to \hat{Y}(p) \approx 1/(1 - 2p)$ as $N \to \infty$. However, we do have to exercise a certain degree of caution in applying this formula. In Fig. 6(b) we present $\hat{Y}(N, p)$ as a function of p as $p \to 1/2$, showing the limiting value $\hat{Y}(p)$ of $\hat{Y}(N, p)$ as N is increased to infinity. We see in this figure that whilst the estimate $\hat{Y}(p) \sim (1 - 2p)^{-2}$ is fairly accurate, a much better estimate in the limit of $p \to 1/2$ is given by $\hat{Y}(p) \sim (1 - 2p)^{-2.6}$ which is consistent with known empirical results on percolation [9].

3. Linear circuit analysis

We now analyse the general electrical network model with two types of bond of admittance y_1 and y_2 in respective proportions $1 - p$ and p, and admittance ratio $\mu = y_2/y_1$ with μ either positive or pure imaginary. Our interest will be in finding how the overall admittance of the system varies as μ itself varies, and seeing how this can be determined in terms of the poles and zeros of the admittance function $Y(\mu)$.

3.1. Linear circuit formulation

Consider the 2D N node square lattice network shown in Fig. 1, with all of the nodes on the left-hand side connected via a bus-bar to a time varying voltage $V(t) = Ve^{i\omega t}$ and on the right-hand side via a bus-bar to earth ($V = 0$). We assign a

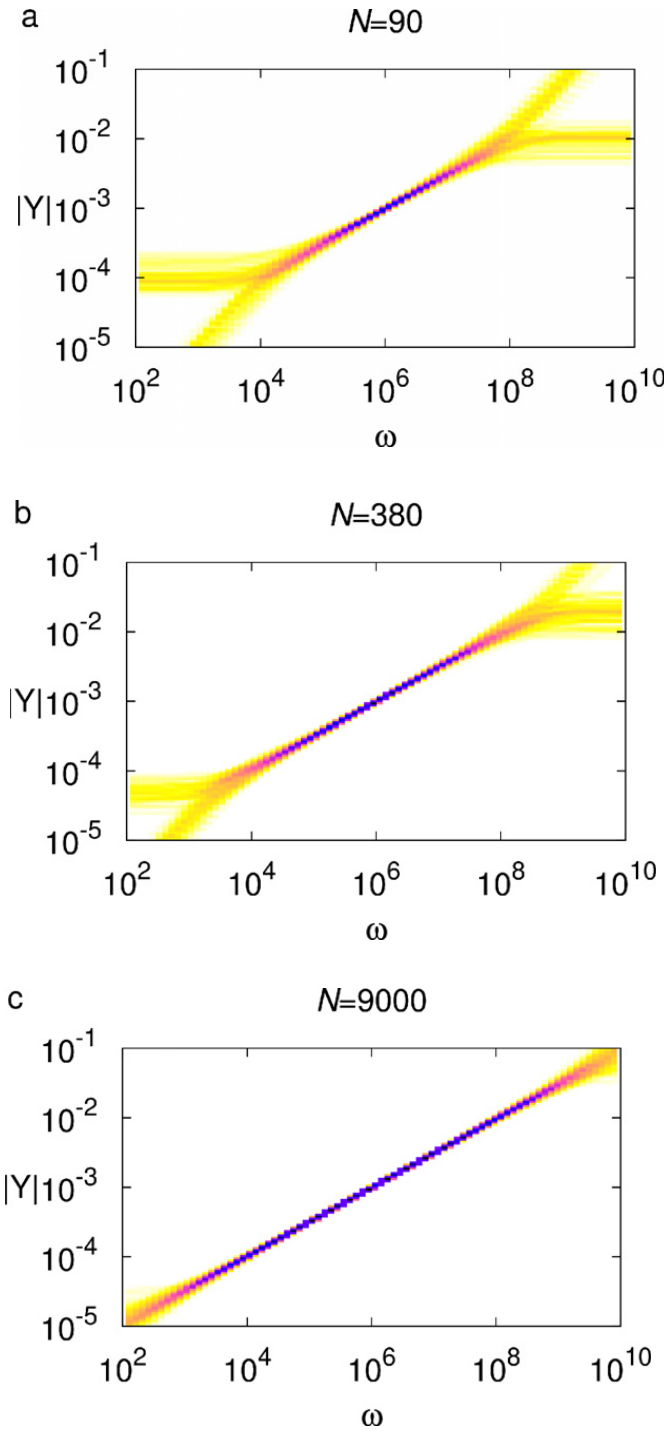

Fig. 4. (Color online) The effect of network size N on the width of the power-law emergent region in the critical case of $p = 1/2$. In this figure we see this region increasing without bound as N increases.

voltage v_i with $i = 1 \cdots N$ to each (interior) node, and set $\mathbf{v} = (v_1, v_2, v_3 \cdots v_N)^T$. We also assume that adjacent nodes are connected by a bond of admittance $y_{\mathrm{i},j} \in \{y_1, y_2\}$. The current from the node i to an adjoining node at j is then given by $I_{\mathrm{i},j}$ where $I_{\mathrm{i},j} = (v_{\mathrm{i}} - v_j)y_{\mathrm{i},j}$. From Kirchhoff's current law, at any interior node all currents must sum to zero, so that

$$\sum_j y_{\mathrm{i},j}(v_{\mathrm{i}} - v_j) = 0. \tag{6}$$

If i is a node adjacent to the *left* boundary then certain of the terms v_j in (6) will take the value of the (known) applied voltage $V(t)$. Similarly, if a node is adjacent to the right-hand boundary then certain of the terms v_j in (6) will take the value of the ground voltage 0. Combining all of these equations together leads to a system of the form

$$K\mathbf{v} = V(t)\mathbf{b} = V\mathrm{e}^{\mathrm{i}\omega t}\mathbf{b}, \tag{7}$$

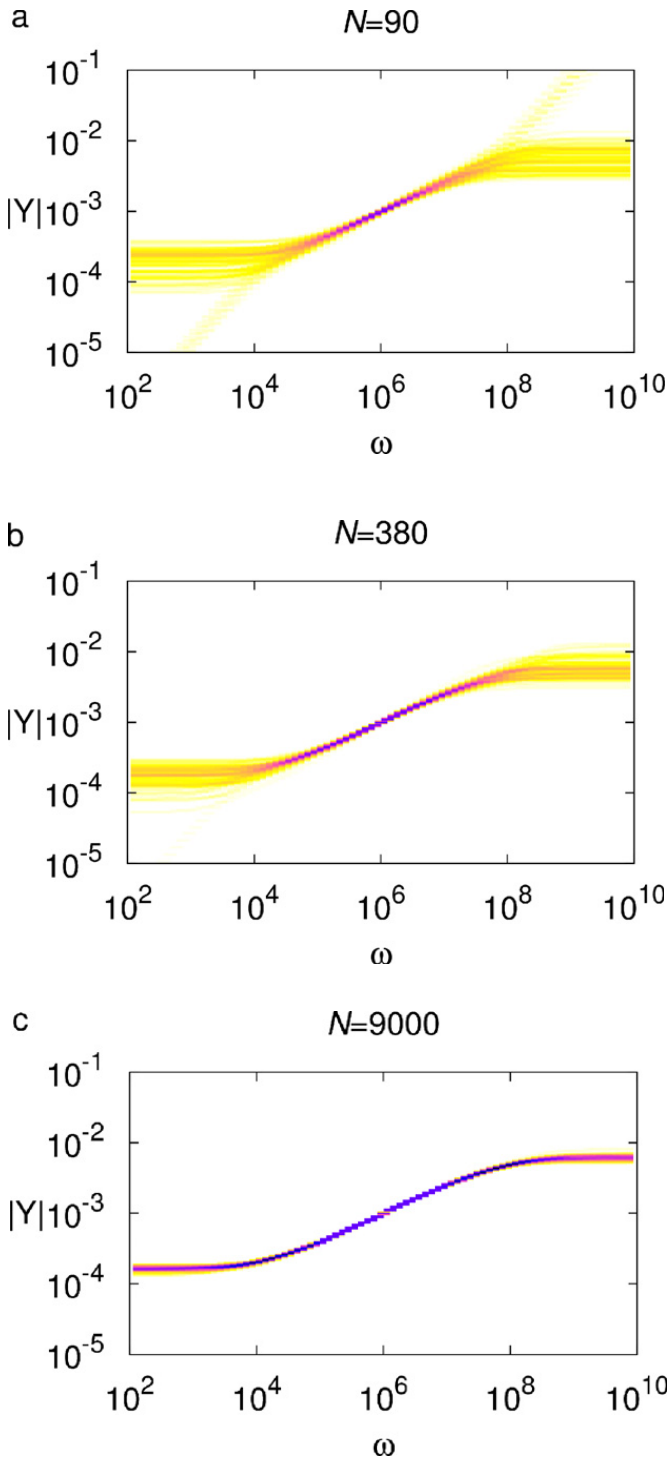

Fig. 5. (Color online) The effect of the network size N on the power-law emergent region for $p = 0.4 < p_c$, in which we see this region becoming asymptotic to a finite set as $N \to \infty$.

where $K \equiv K(\omega)$ is the (constant in time) $N \times N$ *sparse symmetric Kirchhoff matrix* for the system and the adjacency vector $\mathbf{b} \equiv \mathbf{b}(\omega)$ is the vector of the admittances of the bonds between the left-hand boundary and those nodes which connected to this boundary, with zero entries for all other nodes. As this is a *linear system*, we can take $\mathbf{v} = \mathbf{V}e^{i\omega t}$ so that the (constant in time) vector $\mathbf{V}$ satisfies the linear algebraic equation

$$K\mathbf{V} = V\mathbf{b}. \tag{8}$$

If we consider the total current flow I from the LHS boundary to the RHS boundary then we have

$$I = \mathbf{b}^T(V\mathbf{e} - \mathbf{V}) \equiv Vc - \mathbf{b}^T\mathbf{V},$$

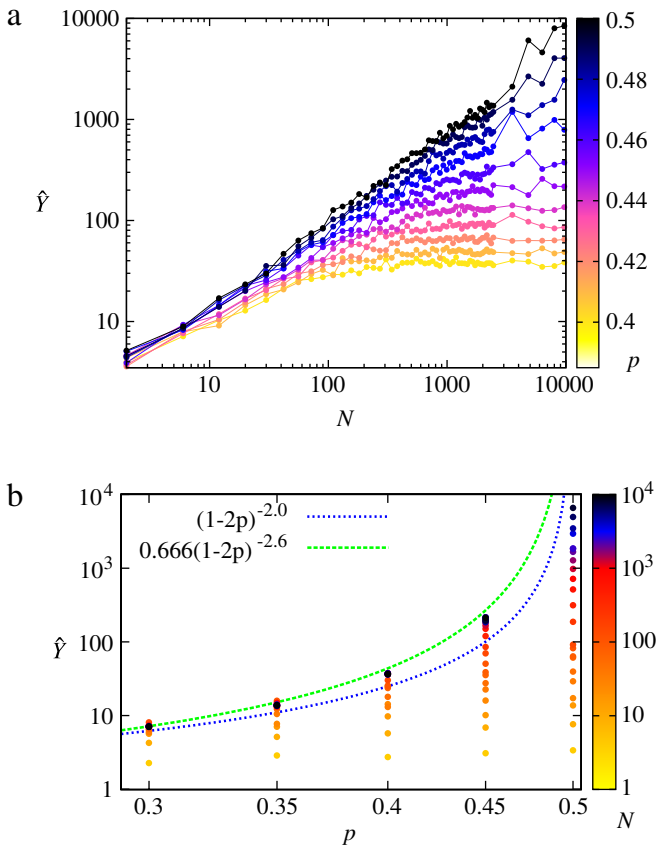

Fig. 6. (Color online) (a) Variation of the dynamic range $\hat{Y} \equiv |Y|_{\max}/|Y|_{\min}$ as a function of N and p, and (b) the value of $\hat{Y}(p)$ as a function of $p \to 1/2$ comparing the estimates $(1-2p)^{-2}$ and $(1-2p)^{-2.6}$. For each value of p the vertical sequence of dots represents calculations of $\hat{Y}$ for increasing values of N.

where $\mathbf{e}$ is the vector comprising ones for those nodes adjacent to the left boundary and zeroes otherwise, and $c = \mathbf{b}^T\mathbf{e}$. Combining these expressions, the equations describing the system are then given by

$$K\mathbf{V} - \mathbf{b}V \equiv \mathbf{0}, \qquad cV - \mathbf{b}^T\mathbf{V} = I. \tag{9}$$

The *bulk admittance* $Y(\mu)$ of the whole system is then given by $Y = I/V$ so that

$$Y(\mu) = c - \mathbf{b}^T K^{-1}\mathbf{b}. \tag{10}$$

The symmetric Kirchhoff matrix K can be separated into the two sparse symmetric $N \times N$ component matrices $K = K_1 + K_2$ corresponding to the conductance paths along the bonds occupied by each of the two types of components. Furthermore, as $\mu = y_2/y_1$, we have

$$K_1 = y_1 L_1 \quad \text{and} \quad K_2 = y_2 L_2 = \mu y_1 L_2 \tag{11}$$

and hence $K = y_1 L_1 + \mu y_1 L_2$, where the terms of the sparse symmetric connectivity matrices L_1 and L_2 are constant and take the values $1, 0, -1$. Note that K is a *linear affine function* of μ. Furthermore, $\Delta = L_1 + L_2$ is the discrete, positive definite symmetric, *negative Laplacian* for a 2D lattice. Similarly we can decompose the adjacency vector into two components $\mathbf{b}_1$ and $\mathbf{b}_2$ so that

$$\mathbf{b} = \mathbf{b}_1 + \mathbf{b}_2 = y_1\mathbf{e}_1 + y_2\mathbf{e}_2 = y_1\mathbf{e}_1 + \mu y_1\mathbf{e}_2,$$

where $\mathbf{e}_1$ and $\mathbf{e}_2$ are *orthogonal vectors* comprising ones and zeros only corresponding to the two bond types adjacent to the LHS boundary. Observe again that $\mathbf{b}$ is a linear affine function of μ. A similar decomposition can be applied to the scalar $c = y_1 c_1 + \mu y_1 c_2$.

3.2. Poles and zeros

As the matrix K, the adjacency vector $\mathbf{b}$ and the scalar c are all affine functions of the parameter μ it follows immediately from (10) and Cramer's rule applied to (9) that the network admittance $Y(\mu)$ is a *rational function* of μ, which is the ratio of two complex polynomials $P(\mu)$ and $Q(\mu)$ of respective degrees $r \leq N$ and $s \leq N$, so that

$$Y(\mu) = \frac{Q(\mu)}{P(\mu)} = \frac{q_0 + q_1\mu + q_2\mu^2 + \cdots + q_r\mu^r}{p_0 + p_1\mu + p_2\mu^2 + \cdots + p_s\mu^s}. \tag{12}$$

We require that $p_0 \neq 0$ so that the response is physically realisable, with $Y(\mu)$ bounded as $\mu \to 0$. Several properties of the network can be deduced from this formula. For convenience, we look at a C–R network with $\mu = \mathrm{i}\omega CR$, although similar results arise for R–R networks. First consider the case of ω *small*. From the discussions in Section 2, we predict that either there is (a) a resistive percolation path in which case $Y(\mu) \sim \mu^0$ as $\mu \to 0$ or (b) such a path does not exist, so that the conduction is capacitive, with $Y(\mu) \sim \mu$ as $\mu \to 0$. The case (a) arises when $p_0 \neq 0$ and the case (b) when $q_0 = 0$. Observe that this implies that the absence of a resistive percolation path as $\mu \to 0$ is equivalent to the polynomial $Q(\mu)$ *having a zero when* $\mu = 0$. Next consider the case of ω and hence $|\mu|$ large. In this case

$$Y(\mu) \sim \frac{q_r}{p_s}\mu^{r-s} \quad \text{as } \mu \to \infty.$$

This time we may have (c) no capacitive path at high frequency with response $Y(\mu) \sim \mu^0$ as $\mu \to \infty$, or the existence of a capacitive path with $Y(\mu) \sim \mu$. In case (c) we have $s = r$ and $p_r \neq 0$ and in case (d) we have $s = r - 1$ so that we can think of taking $p_r = 0$. Accordingly, we identify four corresponding types of network defined in terms of the percolation paths for low and high frequencies:

(a)	$p_0 \neq 0$
(b)	$p_0 = 0$
(c)	$p_r \neq 0$
(d)	$p_r = 0$

Both the polynomials $P(\mu)$ and $Q(\mu)$ can be factorised by determining their respective roots $\mu_{p,k}$, $k = 1 \cdots s$ and $\mu_{z,k}$, $k = 1 \cdots r$ which are the *poles* and *zeroes* of $Y(\mu)$. We will collectively call these poles and zeroes the *resonances* of the network. Our analysis of the network will rely on determining certain statistical and other properties of these resonances. Note that in case (b) we have $\mu_{z,1} = 0$. Accordingly the network admittance can be expressed as

$$Y(\mu, N) = D(N)\frac{\prod_{k=1}^{r}(\mu - \mu_{z,k})}{\prod_{k=1}^{s}(\mu - \mu_{p,k})}. \tag{13}$$

Here $D(N)$ is a function which does not depend on μ but does depend on the characteristics of the network.

3.3. Location of the resonances

We firstly note that the number r of poles/zeroes can be substantially less than N due to the formation of *clusters* of components in the lattice which are isolated from the boundaries [2]. Such component clusters lead to resonances at infinity or zero, depending on which component the clusters are made of. Comparing (10) and (13), it follows that the poles are the roots of the determinant of the matrix $K = y_1(L_1 + \mu L_2)$. The poles are then -1 times the eigenvalues of the matrix pencil (L_1, L_2), so that $\mu_{p,k}$, and the corresponding vectors $\mathbf{v}_{p,k}$, satisfy the linear equation

$$(L_1 + \mu_{p,k}L_2)\mathbf{v}_{p,k} = 0 \quad \text{with } \mathbf{v}_{p,k} \neq 0. \tag{14}$$

As $L_1 + L_2 = \Delta$ this then implies that

$$(L_1(1 - \mu_{p,k}) + \mu_{p,k}\Delta)\mathbf{v}_{p,k} = 0$$

so that

$$(L_1 + \mu_{p,k}\Delta/(1 - \mu_{p,k}))\mathbf{v}_{p,k} = 0.$$

It follows immediately from the symmetry of L_1 and the fact that Δ is a symmetric positive definite operator, that $\mu_{p,k}/(1-\mu_{p,k})$ is real. The negativity of $\mu_{p,k}$ follows from the fact that the network has a bounded response. Similar reasoning shows that the zeroes $\mu_{z,k}$ are also the eigenvalues of a related matrix pencil $(\hat{L}_1, \hat{L}_2)$, which is a block bordered extension of the original matrix pencil. It follows from this reasoning that the values of $\mu_{z,k}$ are also real and negative and, furthermore, that the *the poles and zeros interlace* (see Ref. [9]) so that

$$\begin{aligned} 0 \geq \mu_{z,1} \geq \mu_{p,1} \geq \mu_{z,2} \geq \mu_{z,2} \cdots \\ \geq \mu_{p,s} (\geq \mu_{z,s+1}). \end{aligned} \tag{15}$$

These results have different interpretations in the cases of an R–R and a C–R network. In an R–R network with conductance ratio $\mu > 0$ the poles and zeros occur along the *negative real axis* so that $\mu_{p,k} = -M_{p,k} < 0$, etc. Thus, as μ varies through positive real values

$$Y(\mu) = D(N)\frac{\prod_{k=1}^{r}(\mu + M_{z,k})}{\prod_{k=1}^{s}(\mu + M_{p,k})}, \tag{16}$$

with the values $M_k^z \geq 0$ and $M_k^p > 0$. For the C–R network, $\mu = \mathrm{i}\omega CR$, and Y can be considered a function of ω. The poles $\omega_{p,k}$ of $Y(\omega)$ then satisfy $\mathrm{i}CR\omega_{p,k} = -M_{p,k}$ so that they lie along the positive imaginary axis, as do the zeros. As ω varies through real values then

$$Y(\omega) = D(N)\frac{\prod_{k=1}^{r}(\omega - \mathrm{i}W_{z,k})}{\prod_{k=1}^{s}(\omega - \mathrm{i}W_{p,k})}, \tag{17}$$

with $W_k^z \geq 0$ and $W_k^p > 0$. We note that neither of the expressions (17) and (16) become unbounded as ω varies through real values or as μ varies through positive real values. This is in contrast to the case of a C–L network in which the resonances can be real and positive and can lead to unbounded responses as ω varies. In contrast, we see in the C–R and R–R networks, an averaging effect in the product terms in these expressions, which leads to the observed emergent behaviours.

4. The distribution of the resonances

We now look at the distribution of the poles and zeros, and draw certain conclusions about their statistical regularity, spacing and symmetries which allows us to compute the asymptotic form of the system response. The statistics of the resonances are most regular in the critical case of $p = 1/2$, allowing us to make very precise estimates of the overall system behaviour in this case, precisely complementing the averaging methods which work best when $p \neq 1/2$. To perform these calculations, we note that if we consider the elements of the network to be assigned randomly, with the components taking each of the two possible values with probabilities p and $(1-p)$, then we can consider the resonances to be random variables. The poles and associated eigenvectors are given by the solutions of the matrix pencil equation (14):

$$L_1\mathbf{v}_{p,k} = -\mu_{p,k}L_2\mathbf{v}_{p,k}. \tag{18}$$

Each realisation of the network, with bonds chosen from a Binomial $[p, (1-p)]$ distribution will give a different set of values for $\mu_{p,k} \equiv -\mathrm{i}M_{p,k} \equiv \mathrm{i}CRW_{p,k}$ and we can then consider the statistics of this set. We ask the following questions. (1) What is the statistical distribution of $\mu_{p,k}$ if N is large? (2) What is the statistical distribution of the location of a zero between its two adjacent poles? (3) How do $\mu_{p,1}$ and $\mu_{p,N}$ vary with (large) N? In each case we will find good numerical evidence for strong statistical regularity of the poles (especially in the case of $p = 1/2$), leading to answers to each of the above questions.

4.1. Preliminary observations on the pole locations

When $p = 1/2$ the matrices L_1 and L_2 representing the connectivity of the two components have a statistical duality so that any realisation which leads to a particular matrix L_1 is equally likely to lead to the same matrix L_2. Because of this, if μ is an observed eigenvalue of the pair (L_1, L_2) it is equally likely for there to be an observed eigenvalue $1/\mu$ of the pair (L_2, L_1) with the same eigenvector. Thus in any set of realisations of the system with $p = 1/2$ we will see eigenvalues (and hence poles or zeros) μ and $1/\mu$ occurring with equal likelihood. More generally, if an eigenvalue μ occurs in a realisation with proportion p of component y_2, then we will see an eigenvalue $1/\mu$ in a realisation with proportion $1-p$. It follows from this simple observation that when $p = 1/2$ the variable $\log(\mu)$ should be expected to be a random variable with a symmetric probability distribution and with mean zero. It is therefore natural to expect that for a large number of realisations, the variables $\log(M_{k,p})$ should follow a normal distribution with mean zero (so that $M_{p,k}$ has a log-*normal* distribution centred on $M = 1$). Similarly, if $M_{p,1}$ is the smallest value of $M_{p,k}$ and $M_{p,N}$ the largest value then $M_{p,1} = 1/M_{p,N}$. It follows similarly that $\log(W_{p,k})$ is expected to have a mean value of $-\log(CR)$. Following this initial discussion, we now consider some numerical computations of the distribution of the poles in a C–R network for which $CR = 10^{-6}$. As a first computation we consider many random realisations of networks generated with a large enough size (typically $N = 380$) to ensure good statistics per network. We define S as the number of horizontal components in one row of the network; giving S^2 horizontal and $(S-1)^2$ vertical components. The number of internal nodes (i.e. not including the boundary nodes), which is equal to the dimension of the matrix K, is therefore $N = S(S-1)$; giving the maximum possible number of eigenvalues μ_i. The results of the computations are presented in Fig. 7 in which we give a histogram of the distribution of the poles $W_{p,k}$ (on a log-scale in the frequency domain) over 100 different realisations of each network. These figures clearly indicate that the location of the poles does indeed possess a strong statistical regularity, conforming approximately to a log-*normal distribution* with mean $\log(1/CR)$ in all cases. Evidence for this is given by comparing the resulting curve with the standard Normal distribution with an appropriately chosen value for the variance. The fitted curves in Fig. 7 show that the results are close to log-normal for any choice of p (provided that N is chosen sufficiently large). When the results of the realisations considered above are fitted to a log-normal distribution with probability density function $P(W) = a\exp\left(-(W - E\{W\})^2/2\sigma^2\right)$ we find the remarkable result that the standard deviation σ appears to be largely *independent of the value of* N and to display a simple functional relation on p, with a good fit to the curve $\sigma = \alpha p(1-p)$, over many values of N. As a second calculation we take a *single realisation* of a network with $N \approx 380$ nodes and $p = 1/2$ and determine the location of $W_{p,k}$. A plot of the logarithm of the poles, ordered in increasing size, as a function of k is given in Fig. 8. Two features of this figure are immediately obvious.

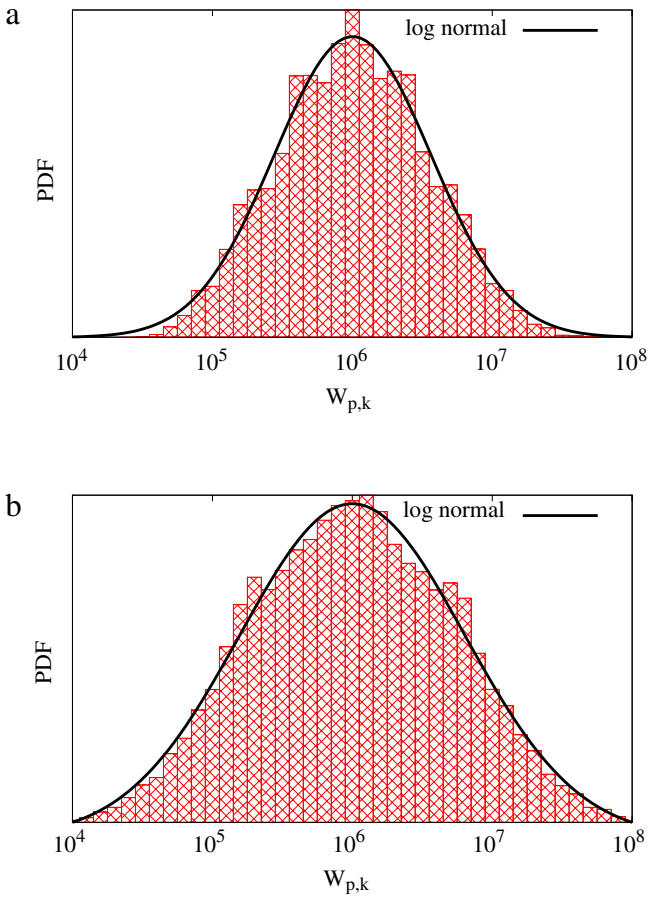

Fig. 7. (Color online) Distribution of $W_{p,k}$ values for (a) $p = 0.25$ and (b) $p = 0.5$ with $N = 380$. The curves are fitted to Normal distributions (on a log-scale). The variance depends on p but is largely independent of the value of N.

Firstly, the terms $W_{p,k}$ appear to be point values of a regular function $f(k)$. Secondly, $\log(CRW_{p,k})$ shows a strong degree of symmetry about zero, so that if $1 \leq k \leq N$ then $\log(CRW_{p,k}) = 0$ if $k = N/2$. Motivated by the discussion above, we compare the form of this graph with that of the *error function*, that is we compare $\mathrm{erf}(\log(CRW_{p,k}))$ with $2k/N - 1$. The correspondence is very good, strongly indicating that $\log(f)$ takes the form of the inverse error function with an appropriate constant of proportionality.

4.2. Pole-zero spacing

As a next calculation we consider the statistical distribution of the location of the interlacing zeros with respect to the poles. In particular we consider the variable η_k, which depends on the proportion p given by

$$\eta_k(p) \equiv \frac{\log M_{p,k+1} - \log M_{z,k}}{\log M_{p,k+1} - \log M_{p,k}} \equiv \frac{\log W_{p,k+1} - \log W_{z,k}}{\log W_{p,k+1} - \log W_{p,k}}. \tag{19}$$

We now establish three symmetry results for the mean value $\bar{\eta}_k(p)$ of η_k, taken over many realisations.

First symmetry: Assume that when the proportion is p that the zeros are $M_{z,k}$, $k \in [0, N]$ and the poles are $M_{p,k}$, $k \in [1, N]$ and when it is $1 - p$ they are $\hat{M}_{z,k}$ and $\hat{M}_{p,k}$, $k \in [1, N]$. Then

$$\eta_k(1-p) \equiv \frac{\log \hat{M}_{p,k+1} - \log \hat{M}_{z,k}}{\log \hat{M}_{p,k+1} - \log \hat{M}_{p,k}}. \tag{20}$$

By the statistical symmetry results described above we have

$$\log \hat{M}_{z,k} = -\log M_{z,N-k}, \qquad \log \hat{M}_{p,k} = -\log M_{p,N-k+1}. \tag{21}$$

So that

$$\eta_{N-k}(1-p) \equiv \frac{\log W_{z,k} - \log W_{p,k}}{\log W_{p,k+1} - \log W_{p,k}}. \tag{22}$$

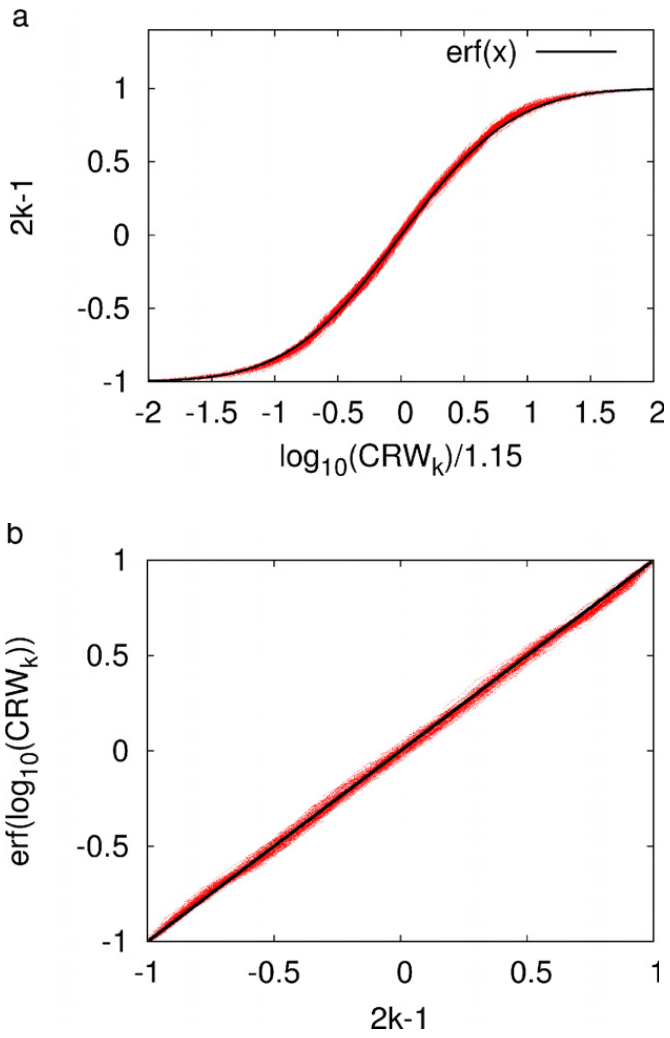

Fig. 8. (Color online) The location of the logarithm of the poles as a function of k, for a single realisation of the network, and a comparison with the inverse error function.

Hence,

$$\eta_k(p) + \bar{\eta}_{N-k}(1-p) = 1. \tag{23}$$

Second symmetry: We next invoke duality results due to Keller [10] (see also Ref. [9]), in which the admittance of a network is compared with that of the dual network, in which every bond of the original network is replaced with an orthogonal bond for the dual. Significantly, square binary networks are self-dual. A consequence of the duality results is that

$$Y(y_1, y_2)\, Y(y_2, y_1) = y_1\, y_2. \tag{24}$$

It follows from (24) that

$$D(N)\frac{\prod_{k=1}^{r}(\mu + M_{z,k})}{\prod_{k=1}^{s}(\mu + M_{p,k})} = \frac{y_1 y_2}{D(N)}\frac{\prod_{k=1}^{s}(1/\mu + M_{p,k})}{\prod_{k=1}^{r}(1/\mu + M_{z,k})}.$$

This can only be true for all μ if we have the symmetry result (taking the ordering of the poles and zeros into account) given by $M_{p,k} = 1/M_{z,N-k}$. It immediately follows from (19) that asymptotically we have the second symmetry

$$\bar{\eta}_k(p) = \bar{\eta}_{N-k}(p). \tag{25}$$

Third symmetry: Combining (23) and (25), we have

$$\bar{\eta}_k(p) + \bar{\eta}_k(1-p) = 1. \tag{26}$$

In particular, this gives

$$\bar{\eta}_k(1/2) = 1/2. \tag{27}$$

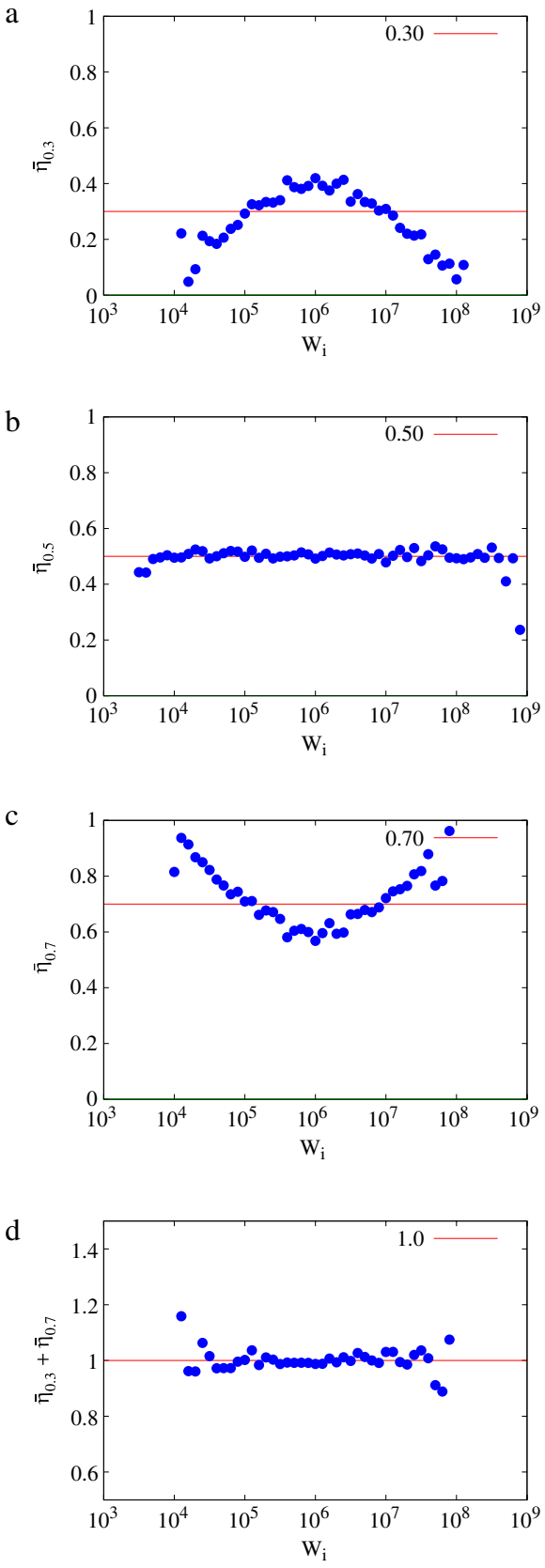

Fig. 9. (Color online) Figures showing how the mean value $\bar{\eta}_k$ of η_k taken over many realisations of the network, varies with the mean value of $W_{p,k}$. The four examples show results for (a) $p = 0.3$, (b) $p = 0.5$, (c) $p = 0.7$ and (d) $\bar{\eta}(0.3) + \bar{\eta}(0.7)$.

The distribution of $\bar{\eta}_k(p)$ over 100 *realisations* of a C–R network, plotted as a function the location of $\log(W_{p,k})$ for $p = 0.3, 0.5, 0.7$, is shown in Fig. 9 together with a graph of $\bar{\eta}_k(0.3) + \bar{\eta}_k(0.7)$. Figures (a)–(c) show clearly the reflectional symmetry about the mid-point implied by (25). The figure in part (b) (with $p = 1/2$) is particularly remarkable, showing, as

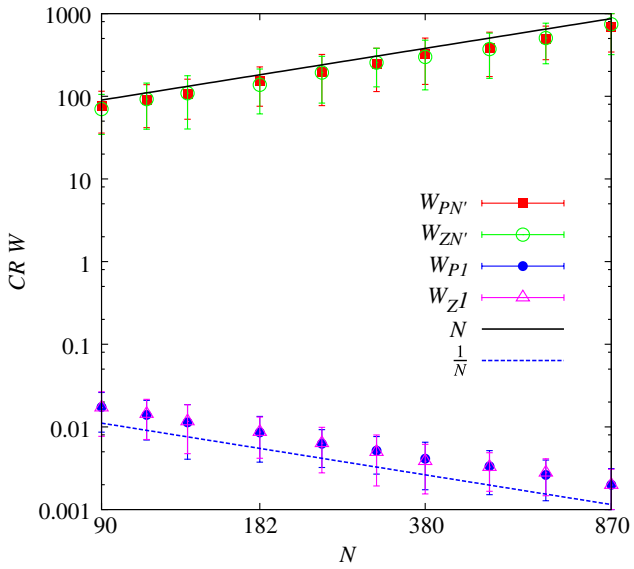

Fig. 10. (Color online) Largest $W_{z,N'}$, $W_{p,N'}$ and smallest $W_{z,1}$, $W_{p,1}$ zeros and poles for a C–R network with $p = 0.5$ showing linear dependence on N and $1/N$.

predicted by (27) that $\bar{\eta}_k(1/2)$ is equal to $1/2$ almost independently of the value of $\log(W_{p,k})$. There is some deviation from this value at the high and low ends of the range due to slower convergence to the mean. The figure in part (d) for $p = 0.3$ and $p = 0.7$ also clearly illustrates the symmetry relation (26). We note, however, that for $p \neq 1/2$ the value of $\bar{\eta}_k$ of η_k varies with $\log(W_{p,k})$ in a symmetric distribution (as predicted by (25)) which depends approximately quadratically on the value of $\log(W_{p,k})$. If $p > 1/2$, $\bar{\eta}_k$ takes a value a little less than p in the centre of the range when $W_{p,k} = W_{mid} = 1/CR$, and a bit greater than p towards the ends of the range. The distribution is reversed when $p < 1/2$, as can be seen by comparing Fig. 9(a) and (c), and this is a consequence of (26).

4.3. Limits of the resonance distributions

As a final calculation, we consider the number N' of the *finite non-zero resonances* in this case of a C–R network, and the location of the first non-zero pole and zero $W_{z,1}$, $W_{p,1}$ and the last finite pole and zero $W_{p,N'}$, $W_{z,N'}$. As discussed, in the case of $p = 1/2$ we expect a symmetrical relation so that $CRW_{p,1}$ and $CRW_{p,N'}$ might be expected to take reciprocal values. We consider two calculations, firstly determining N'/N for a range of values of N and of p and secondly calculating the functional dependence of $W_{p,1}$ and $W_{p,N'}$ upon N and p. The value of N' can be considered statistically and represents probability of a node contributing to the current paths. If we take $z = N'/N$ as a function of p for a range of values of N the shape of this curve is parabolic in p with a maximum value for $z \approx 0.8$ given when $p = 1/2$, consistent with statistical arguments presented in Ref. [9], which imply that the maximum value at $p = 1/2$ is given by $N' = 3\left(2 - \sqrt{3}\right) = 0.804\cdots$. We next consider the values of $W_{p,1}$ and of $W_{p,N'}$ which will mark the transition between emergent type behaviour and percolation type behaviour. A log–log plot of the values of $W_{z,1}$, $W_{p,1}$ and of $W_{z,N'}$, $W_{p,N'}$ as functions of N for the case of $p = 1/2$ is given in Fig. 10. There is very clear evidence from these plots that each of $W_{z,1}$, $W_{p,1}$ and $W_{z,N'}$, $W_{p,N'}$ both have a *strong linear dependence* upon N and $1/N$ for *all values of* N. Indeed we conclude from this figure that the following reciprocal relations hold

$$CR\ W_{z,1},\ CR\ W_{p,1} \sim N^{-1}$$

and

$$CR\ W_{z,N'},\ CR\ W_{p,N'} \sim N,$$

with an identical scaling for $M_{z,1}$, $M_{p,1}$, $M_{z,N'}$, $M_{p,N'}$.

4.4. Summary

The main conclusions of this section are that there is a strong statistical regularity in the location of the poles and the zeros of the admittance function.

1. $M_{p,k} \sim f(k)$ for an appropriate continuous function $f(k)$ where f depends upon p strongly and upon N very weakly.
2. $\bar{\eta}_k(1/2) \approx 1/2$ for all values of k.
3. If $p = 1/2$ and $M_{z,1} \neq 0$, then

$$M_{p,1},\ M_{z,1} \sim N^{-1}, \qquad M_{p,N'},\ M_{z,N'} \sim N.$$

5. Asymptotic analysis of the conductance when $p = 1/2$ using spectral arguments

5.1. Derivation of the response for general μ

We consider the formulae for the value of the admittance of the binary network

$$Y(\mu) = D(N)\frac{\prod_{k=1}^{r}(\mu - \mu_{z,k})}{\prod_{k=1}^{s}(\mu - \mu_{p,k})}, \tag{28}$$

where the results of Section 3 imply that $\mu_{z,k} = -M_{z,k}$, and $0 \leq M_{z,1} < M_{p,1} < M_{z,2} < M_{p,2} < \cdots < M_{p,s} (< M_{z(s+1)})$. As μ is either positive or purely imaginary, Y is a *bounded function* for all μ. Here we assume that we have $s = N'$ poles, but consider situations with different percolation responses for $|\mu|$ large or small, depending upon whether the first zero $M_{z,1} = 0$ and on the existence or not of a final zero $M_{z,(N'+1)}$. These four cases lead to four functional forms for the conductance, all of which are realisable in the case of $p = 1/2$ and we derive each of these from asymptotic arguments. At this stage the constant $D(N)$ is undetermined, but we will be able to deduce its value from our subsequent analysis. Although simple, these arguments lead to remarkably accurate formulae when compared with the numerical calculations, that predict not only the PLER but also the limits of this region. To obtain an asymptotic formula from (28) we assume that $s = N'$ is large, and that there is a high density of poles and zeros. From the results in the previous section we know that, asymptotically, the poles at $-M_{p,k}$ follow a regular distribution and that the zeroes have a regular spacing between the poles. From the previous section we have $M_{p,k} \sim f(k)$ so that $M_{p,k+1} - M_{p,k} \sim f'(k)$. Setting

$$\frac{M_{p,k+1} - M_{z,k+1}}{M_{p,k+1} - M_{p,k}} = \delta_k$$

we have

$$M_{z,k+1} \sim f(k) + (1 - \delta_k)f'(k). \tag{29}$$

As we have seen, the function $\log(f(k))$ is given by the inverse of the error function, but its precise form does not matter too much for the next calculation. To do this we firstly consider the contributions to the product in (28) which arise from the terms from the first pole to the final zero:

$$P \equiv D(N)\prod_{k=1}^{N'}\frac{\mu + M_{z,k}}{\mu + M_{p,k}}. \tag{30}$$

Note that this product has implicitly assumed the existence of a final zero $M_{z,(N'+1)}$, specific to the case where there is a percolation path through the y_2 bonds but no percolation path through the y_1 bonds. This contribution will be corrected in cases for which such a final zero does not exist. Using the results in (29), in particular on the mean spacing of the zeros between the poles, we may express P as

$$\begin{aligned} P &= D(N)\prod_{k=1}^{N'}\frac{\mu + (f(k) + (1 - \bar{\delta}_k)f'(k))}{\mu + f(k)} \\ &= D(N)\prod_{k=1}^{N'}1 + \frac{(1 - \bar{\delta}_k)f'(k)}{\mu + f(k)}. \end{aligned}$$

Taking the logarithm of both sides and using the approximation $\log(1 + x) \approx x$ for small x, we have

$$\log(P) \approx \log(D(N)) + \sum_{k=1}^{N'}\frac{(1 - \bar{\delta}_k)f'(k)}{\mu + f(k)}. \tag{31}$$

We now approximate the sum in (31) by an integral, so that

$$\log(P) \approx \log(D(N)) + \int_{k=1}^{N'}(1 - \bar{\delta}_k)\frac{f'(k)}{\mu + f(k)}\,\mathrm{d}k.$$

Making a change of variable from k to f, gives

$$\log(P) \approx \log(D(N)) + \int_{M_{p,1}}^{M_{p,N'}}(1 - \bar{\delta}(f))\frac{\mathrm{d}f}{\mu + f}. \tag{32}$$

5.2. The asymptotic form of the equations when $p = 1/2$

To proceed we first determine the relation between η_k and δ_k. Let

$$\delta M_{p,k} = M_{p,k+1} - M_{p,k}$$
$$\delta \log M_{p,k} = \log M_{p,k+1} - \log M_{p,k}.$$

As $M_{z,k} = (1-\delta_k)\delta M_{p,k} + M_{p,k}$, we have

$$\log M_{z,k} = \log\big((1-\delta_k)\delta M_{p,k}/M_{p,k} + 1\big) + \log M_{p,k}.$$

Comparing with the exact expression

$$\log M_{z,k} = (1-\eta_k)\delta \log M_{p,k} + \log M_{p,k},$$

and taking Taylor expansions, we have

$$(1-\eta_k)\sum_{j=1}^{\infty} \frac{(-1)^{j+1}}{m!}\left(\frac{\delta M_{p,k}}{M_{p,k}}\right)^j = \sum_{j=1}^{\infty}(1-\delta_k)^j \frac{(-1)^{j+1}}{j!}\left(\frac{\delta M_{p,k}}{M_{p,k}}\right)^j. \tag{33}$$

When $(\delta M_{p,k}/M_{p,k})^2 \ll (\delta M_{p,k}/M_{p,k})$ it follows that

$$\eta_k \approx \delta_k.$$

Assuming the poles have a log-normal distribution then $\delta \log M_{p,k} \sim O(1/N)$. For a sufficiently large network, when $p = 0.5$, we expect $\delta_k \approx \eta_k$ for most k (the first order Taylor expansion becomes invalid near the tails of the normal distribution, but this contributes relatively little to the summation in (31)). The results imply that $\bar{\delta}_k$ is very close to being constant at $1/2$, so that in (32) we have $1 - \bar{\delta} = 1/2$. We can then integrate the expression for P exactly. This allows sharp estimates of the asymptotic behaviour in this critical case. Integrating (32) gives

$$\log(P) \approx \log(D(N)) + \frac{1}{2}\log\left(\frac{\mu + M_{p,N'}}{\mu + M_{p,1}}\right),$$

so that

$$P \approx D(N)\left(\frac{\mu + M_{p,N'}}{\mu + M_{p,1}}\right)^{\frac{1}{2}}.$$

In this *critical case* it is equally likely that we will/will not have percolation paths along y_1 or y_2 bonds at both small and large values of $|\mu|$. Accordingly, we must consider four equally likely cases of the distribution of the poles and zeros which could arise in any random realisation of the network. Thus to obtain the four possible responses of the network we must now consider the contribution of the first zero and also of the last zero.

Case 1: first zero at the origin, last zero at $N' + 1$. This corresponds to there being a percolation path through the y_2 bonds. To determine this case we multiply P by μ to give $Y_1(\mu)$ so that

$$Y_1(\mu) \approx D(N)_1\, \mu\left(\frac{\mu + M_{p,N'}}{\mu + M_{p,1}}\right)^{\frac{1}{2}}. \tag{34}$$

Case 2: first zero not at the origin, last zero at $N'+1$. This corresponds to the existence of percolation paths through y_1 bonds and y_2 bonds. In this case we multiply P by $\mu + M_{z,1}$ to give $|Y(\mu)|$. We also use the result from the previous section that asymptotically $M_{z,1} \sim M_{p,1}$. This then gives

$$Y_2(\mu) \approx D(N)_2\left(\mu + M_{p,N'}\right)^{\frac{1}{2}}\left(\mu + M_{p,1}\right)^{\frac{1}{2}}. \tag{35}$$

Case 3: first zero at the origin, last zero at N'. Here there are no percolation through either set of bonds. To determine this case we multiply P by μ and divide by $\mu + M_{z,N'}$ to give Y. Exploiting the fact that asymptotically $M_{p,N'} \sim M_{z,N'}$ we then have

$$Y_3(\mu) \approx D(N)_3\, \frac{\mu}{\left(\mu + M_{p,N'}\right)^{\frac{1}{2}}\left(\mu + M_{p,1}\right)^{\frac{1}{2}}}. \tag{36}$$

Case 4: first zero not at the origin, last zero at N'. This final case there exists percolation via the y_1 bonds but not through the y_2 bonds. To determine this case we multiply P by $\mu + M_{z,1}$ and divide by $\mu + M_{z,N'}$ to give Y. Again, exploiting the fact that asymptotically $W_{p,N'} \sim W_{z,N'}$ we have

$$Y_4(\mu) \approx D(N)_4\left(\frac{\mu + M_{p,1}}{\mu + M_{p,N'}}\right)^{\frac{1}{2}}. \tag{37}$$

We know, further, from the calculations in the previous section that for all sufficiently large values of N

$$M_{p,1} \sim 1/N \quad \text{and} \quad M_{p,N'} \sim N.$$

Substituting these values into the expression for Y_1 gives

$$Y_1(\mu) \approx D(N)_1 \, \mu \left(\frac{\mu + N}{\mu + 1/N} \right)^{\frac{1}{2}}. \tag{38}$$

The value of the constant $D(N)_1$ can be determined by considering the mid-range of each of these expressions. The results of the classical Keller duality theory [10] predict that each of the expressions Y_i takes the same form in the range $1/N \ll |\mu| \ll N$ with

$$Y_{\mathrm{i}}(\mu) \approx \sqrt{y_1 y_2}, \quad \mathrm{i} = 1, 2, 3, 4. \tag{39}$$

In the case of Y_1 we see that the mid-range form of the expression (38) is given by $Y_1 = D_1\sqrt{N\mu} = \sqrt{N}\sqrt{y_2}/\sqrt{y_1}$. This then implies that $D_1 = y_1/\sqrt{N}$ so that

$$Y_1(\mu) \approx \frac{y_1 \, \mu}{\sqrt{N}} \left(\frac{\mu + N}{\mu + 1/N} \right)^{\frac{1}{2}}. \tag{40}$$

Very similar arguments lead to the following expressions in the other three cases:

$$Y_2(\mu) \approx \frac{y_1}{\sqrt{N}} \, (N + \mu)^{\frac{1}{2}} \, (1/N + \mu)^{\frac{1}{2}}, \tag{41}$$

$$Y_3(\mu) \approx \sqrt{N} y_1 \, \frac{\mu}{(N + \mu)^{\frac{1}{2}} \, (1/N + \mu)^{\frac{1}{2}}}, \tag{42}$$

$$Y_4(\mu) \approx \sqrt{N} y_1 \left(\frac{1/N + \mu}{N + \mu} \right)^{\frac{1}{2}}. \tag{43}$$

The four formulae above give a very complete asymptotic description of the response of the binary network when $p = 1/2$. In particular they allow us to see the transition between the power-law emergent region and the percolation regions and they also describe the form of the expressions in the percolation regions. We see a clear transition between the emergent and the percolation regions at

$$\mu_1 = 1/N \quad \text{and} \quad \mu_2 = N. \tag{44}$$

Hence, the number of components in the system for $p = 1/2$ has a strong influence on the *boundaries* of the emergent region and also on the *percolation response*. However the emergent behaviour itself is *independent of* N. Observe that these frequencies correspond directly to the limiting pole and zero values. This gives a partial answer to the question of *how large N has to be* to see an emergent response from the network. The answer is that N has to be sufficiently large so that $1/N$ and N are widely separated frequencies. The behaviour in the percolation regions in then given by the following:

$$Y_1(|\mu| \ll 1) \approx y_2\sqrt{N}, \qquad Y_1(|\mu| \gg 1) \approx \frac{y_2}{\sqrt{N}}, \tag{45}$$

$$Y_2(|\mu| \ll 1) \approx \frac{y_1}{\sqrt{N}}, \qquad Y_2(|\mu| \gg 1) \approx \frac{y_2}{\sqrt{N}}, \tag{46}$$

$$Y_3(|\mu| \ll 1) \approx y_2\sqrt{N}, \qquad Y_3(|\mu| \gg 1) \approx y_1\sqrt{N}, \tag{47}$$

$$Y_4(|\mu| \ll 1) \approx \frac{y_1}{\sqrt{N}}, \qquad Y_4(|\mu| \gg 1) \approx y_1\sqrt{N}. \tag{48}$$

We note that these percolation limits, with the strong dependence upon $\sqrt{N}$ are exactly as observed in Section 2.

5.3. The network response when $p \neq 1/2$

This case differs from the case of $p = 1/2$ and the spectral analysis harder and less complete. Rather than getting four different responses we see only two, and the values for the conductance at high and low frequencies are asymptotically independent of (sufficiently large) N. When $p > 1/2$ then there will (with probability one) always be conducting y_2 percolation paths for large values of $|\mu|$ and for small values of $|\mu|$ there is no y_1 percolation path. Similarly, if $p < 1/2$ then we will get (with probability one) a response with no y_2 percolation path at high frequencies and y_1 percolation paths at low frequencies. Hence, we need only consider Cases 1 and 4 respectively. Secondly the formula for P in (32) involves a quadrature involving $1 - \bar{\delta}$ which cannot be obtained in closed form. As a consequence we shall adopt a different approach for $p \neq 1/2$ by combining the spectral calculation with an averaging method.

6. Averaging calculations

The Effective Medium Approximation (EMA) formula derived by an averaging method [4], gives an approximation to the conductance of the network, and is derived by regarding the random distribution of the bonds as a series of perturbations of a uniform field of identical conductors. The conductance of the effective medium is chosen to minimise the first moment of the resulting perturbation matrix. It assumes an infinitely large number of conductances and hence corresponds to taking $N \to \infty$ in the previous analyses. Whilst accurate for p not too close to $1/2$ it has limitations for p close to $1/2$, in that whilst it predicts a transition from emergent to percolation type behaviour, the form of this transition is not quite correct as $p \to 1/2$. Thus the EMA calculations are complementary to those derived using spectral methods in the previous section. In this section we will review the EMA result, and show that it is consistent with a PLER description of the behaviour with a power law which we explicitly derive. Motivated by the spectral calculations, we then extend the EMA formula to include the effects of finite network size N. We see presently that if $N > N^* \equiv |p - 1/2|^{-2}$ then the EMA formula gives a good approximation to the resulting conductance and the extended formula is effective for all $|p - 1/2|$ and $1/\sqrt{N}$ sufficiently small.

6.1. Infinite networks

6.1.1. Overview

If the conductances y_1 and y_2 are in proportion $1 - p$ and p, the 'classical' EMA result in Ref. [4] states that the effective medium conductance Y for a very large ($N \to \infty$) *square two-dimensional lattice* solves the quadratic equation

$$(1-p)\left(\frac{Y-y_1}{Y+y_1}\right) + p\left(\frac{Y-y_2}{Y+y_2}\right) = 0. \tag{49}$$

Rearranging we have

$$Y^2 + (1-2p)(y_2 - y_1)Y - y_1 y_2 = 0,$$

so that if

$$\epsilon = (1-2p), \qquad \theta = Y/\sqrt{y_1 y_2}, \qquad \mu = y_2/y_1,$$

we have

$$\theta - 1/\theta + \epsilon\left(\sqrt{\mu} - 1/\sqrt{\mu}\right) = 0. \tag{50}$$

Setting $\gamma = \log(\theta)$ and $\nu = \log(\mu)$ we have

$$\sinh(\gamma) = -\epsilon \sinh(\nu/2). \tag{51}$$

6.1.2. Emergent power laws

Suppose firstly that μ is *real* and close to unity, so that ν, and hence γ are both not large. Then we may linearise (51) and to leading order have $\gamma = -\epsilon\nu/2$. Thus in this case $\log(Y/\sqrt{y_1 y_2}) = \epsilon \log(y_1/y_2)/2$, and rearranging this gives the elegant power-law identity

$$Y = y_1^{(1-p)} y_2^{p}. \tag{52}$$

This is fully consistent with the duality result (24) that

$$Y(y_1, y_2)Y(y_2, y_2) = y_1^{(1-p)} y_2^{p} y_1^{p} y_2^{(1-p)} = y_1 y_2.$$

In a C–R network, $\mu = \mathrm{i}\omega CR$ is *pure imaginary*. We set $\mu = \mathrm{i}\eta$ where $\eta = \omega CR$ is now assumed to be close to unity and take $\beta = \log(\eta)$ to be close to zero. It then follows that $\log(\mu) = \mathrm{i}\pi/2 + \beta$ so that

$$\sinh(\gamma) = -\epsilon \sinh(\mathrm{i}\pi/4 + \beta/2) = -\epsilon(\mathrm{i} + \beta/2 + \mathcal{O}(\beta^2))/\sqrt{2}.$$

If $\beta = 0$ then $\gamma = \mathrm{i}\theta_0$ where $\sin(\theta_0) = -\epsilon/\sqrt{2}$. Linearising about this solution we have, to leading order,

$$\gamma = \mathrm{i}\theta_0 - \frac{\epsilon}{2\sqrt{2}\cos(\theta_0)}\beta + \mathcal{O}(\beta^2) \equiv \mathrm{i}\theta_0 + \Lambda \log(\eta) + \mathcal{O}(\beta^2).$$

Thus, to leading order

$$|Y| = \sqrt{\omega C/R}\,|\exp(\gamma)| = \sqrt{\omega C/R}\,(\omega CR)^{\Lambda} \equiv K\omega^{\alpha}.$$

This gives the power law observed in Section 2 in a frequency range centred around $\omega CR = \mathcal{O}(1)$ and with

$$\alpha(p) = \frac{1}{2} + \Lambda = \frac{1}{2} - \frac{\epsilon}{2\sqrt{2}\sqrt{1-\epsilon^2/2}}. \tag{53}$$

6.1.3. Percolation behaviour

It is well known that the EMA approximation for $p \neq 1/2$ exhibits percolation behaviour which we summarise. If ν is large and positive then the asymptotic form of the solution depends upon the sign of ϵ. If $\epsilon > 0$, which corresponds to $p < 1/2$ then for large α Eq. (51) reduces to $e^{-\gamma} = \epsilon e^{\nu/2}$ so that we have the percolation behaviour given by:

$$1/\theta = \epsilon\sqrt{\mu}, \qquad Y = y_1/\epsilon. \tag{54}$$

In contrast, if $\epsilon < 0$, $(p > 1/2)$ then for large ν Eq. (51) simplifies to: $e^{\gamma} = (-\epsilon)e^{\nu/2}$ so that we have the percolation behaviour given by:

$$\theta = -\epsilon\sqrt{\mu}, \qquad Y = -\epsilon y_2. \tag{55}$$

Similar results for ν large and negative follow from duality arguments. The (frequency) limits of the emergent region can be estimated by finding when the power-law behaviour of (52) overlaps with the percolation type behaviour. This leads to the following estimates for the values $\mu_1 < \mu < \mu_2$ over which we expect to see power-law emergent behaviour

$$\epsilon > 0 : \mu_1 = 1/\mu_2 \sim \epsilon^{1/p}, \qquad \epsilon < 0 : \mu_1 = 1/\mu_2 \sim (-\epsilon)^{1/(1-p)}. \tag{56}$$

Note, these results predict that as $\epsilon \to 0$ the percolation amplitudes scale as $|\epsilon|^{\pm 1}$. In contrast, calculations in Ref. [9] imply instead a scaling law of the form $|\epsilon|^{\pm 1.3}$.

6.2. Large, but finite, networks

We now give a more speculative calculation which combines the EMA estimate with finite size effects and the spectral calculations of the previous section, for Cases 1 and 4. Our starting point is the spectrally derived formula for $Y = Y_1$ (40) which has percolation limits proportional to y_2 when μ is large. Casting Y in terms of y_1 and y_2 we have

$$Y^2 = \frac{\mu^2 y_1^2}{N}\frac{(\mu + N)}{(\mu + 1/N)} = \mu y_1^2 \frac{(1 + \mu/N)}{(1 + 1/N\mu)} = y_1 y_2 \frac{(1 + \mu/N)}{(1 + 1/N\mu)}.$$

It follows that

$$(1 + 1/N\mu)Y^2 - y_1 y_2(1 + \mu/N) = 0.$$

If we again set $\theta = Y/\sqrt{y_1 y_2}$ this formula can be rearranged into the symmetric form

$$\theta - 1/\theta = \frac{1}{N}\left(\mu/\theta - \theta/\mu\right). \tag{57}$$

Similarly, the spectrally derived formula Y_4 in (43), which has percolation limits proportional to y_1 for μ large, takes the symmetric form

$$\theta - 1/\theta = \frac{1}{N}\left(1/\mu\theta - \mu\theta\right). \tag{58}$$

These expressions are both very similar in form to the result (50) of the EMA calculation. We conjecture that a more general expression can be obtained by combining them into the following two formulae which agree with each in the limits of $\epsilon = 0$ and $N = \infty$ and which include both the effects of component proportion and network size and which respectively have percolation limits proportional to y_1 and y_2:

$$\theta - \frac{1}{\theta} + \epsilon\left(\sqrt{\mu} - \frac{1}{\sqrt{\mu}}\right) = \frac{1}{N}\left(\frac{1}{\mu\theta} - \mu\theta\right) \tag{59}$$

and

$$\theta - \frac{1}{\theta} + \epsilon\left(\sqrt{\mu} - \frac{1}{\sqrt{\mu}}\right) = \frac{1}{N}\left(\frac{\mu}{\theta} - \frac{\theta}{\mu}\right). \tag{60}$$

We observe that each of (59) and (60) is *self-dual* under the map $\mu \to 1/\mu, \theta \to 1/\theta$. Similarly the symmetry $\mu \to 1/\mu$, $\epsilon \to -\epsilon$ maps (59)–(60) and vice versa. We now proceed to show that (59) and (60) have the correct asymptotic form of solution and give numerical evidence for their validity in Section 7. We firstly consider the percolation limits of (59) and (60). Motivated by the analysis in the previous subsection we consider solutions of the form $\theta = \beta\sqrt{\mu}$ so that $Y = \beta y_2$, and $\theta = \beta/\sqrt{\mu}$, so that $Y = \beta y_1$, in the two cases of μ large and μ small. If μ is large and $\epsilon > 0$ then (59) has a solution with percolation limit proportional to, and in phase with, y_1, so that $\theta = \beta/\sqrt{\mu}$ if β satisfies the quadratic equation

$$\frac{\beta^2}{N} + \epsilon\beta - 1 = 0. \tag{61}$$

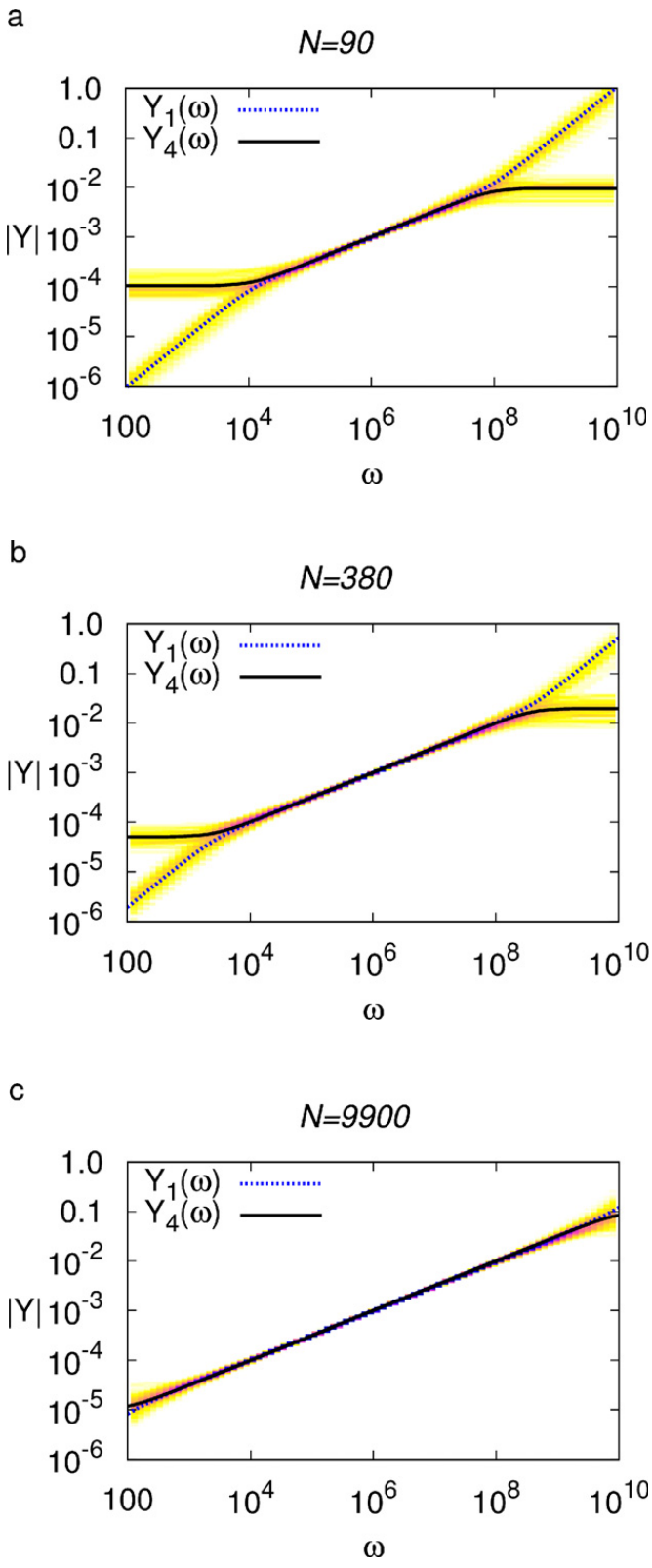

Fig. 11. (Color online) Comparison of the asymptotic formulae obtained from the spectral derivation with the numerical computations for the C–R network over many realisations, with $p = 1/2$ and network sizes $S = 10, 20, 100$, $N = S(S-1)$.

If μ is small then we have the reciprocal solution given by the map $\beta \to 1/\beta$. Note that if $\theta = \beta/\sqrt{\mu}$ then $|Y| = \beta|y_1|$ and hence the dynamic range is given by

$$\hat{Y} = \beta^2 \quad \text{where } \frac{\beta^2}{N} + \epsilon\beta = 1. \tag{62}$$

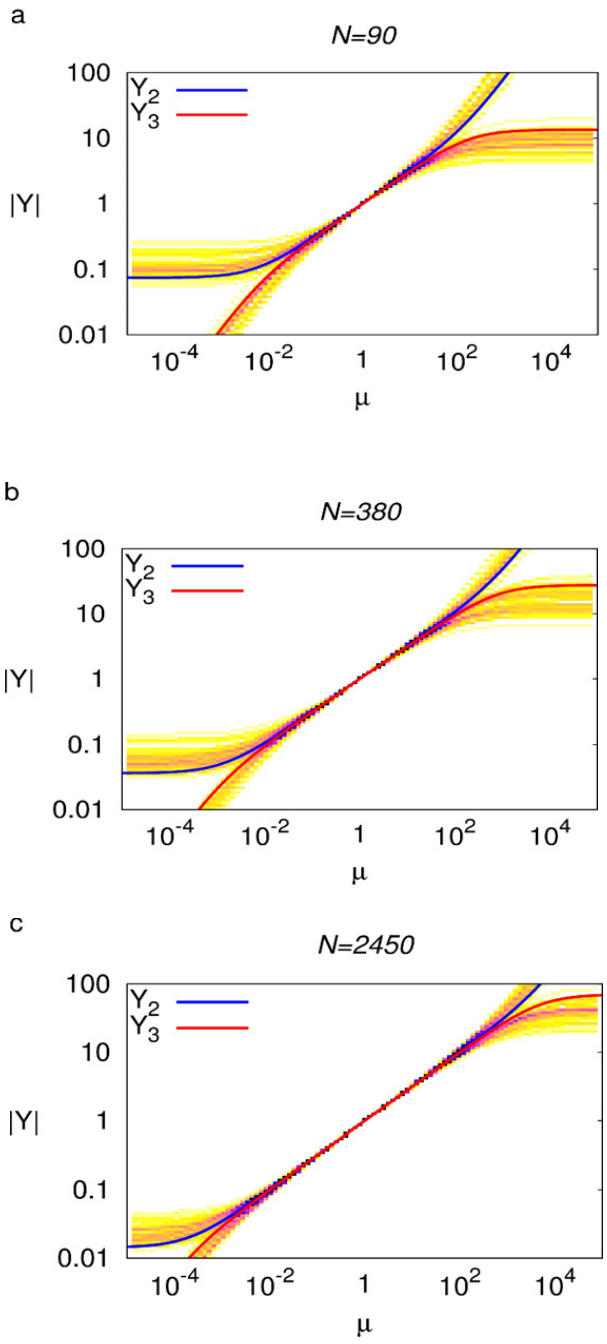

Fig. 12. (Color online) Comparison of the asymptotic formulae with the numerical computations for the *R–R* network over many realisations, with $p = 1/2$ and network sizes $S = 10, 20, 100, N = S(S-1)$.

It is immediate that β is given by

$$\beta = \frac{N}{2}\left(-\epsilon + \sqrt{\epsilon^2 + 4/N}\right), \tag{63}$$

where the positive sign for the square root term is taken to ensure that $\beta > 0$ so that the response is in phase with y_1. This expression takes two different forms depending on whether (i) $N \ll \epsilon^{-2}$ or (ii) $N \gg \epsilon^{-2}$. In the first case the network behaves in a similar way to one with $p = 1/2$ and we have $\beta \sim \sqrt{N}$. In the second case we have behaviour similar to $N = \infty$ with $\beta \sim 1/\epsilon$. This is in exact correspondence with the calculations of the dynamic range reported in Section 2. Similarly, if μ is large and $\epsilon < 0$ then Eq. (60) has a solution with percolation limit proportional to, and in phase with, y_2, so that $\theta = \beta\sqrt{\mu}$, if β satisfies the quadratic equation

$$\beta^2 + \epsilon\beta - \frac{1}{N} = 0. \tag{64}$$

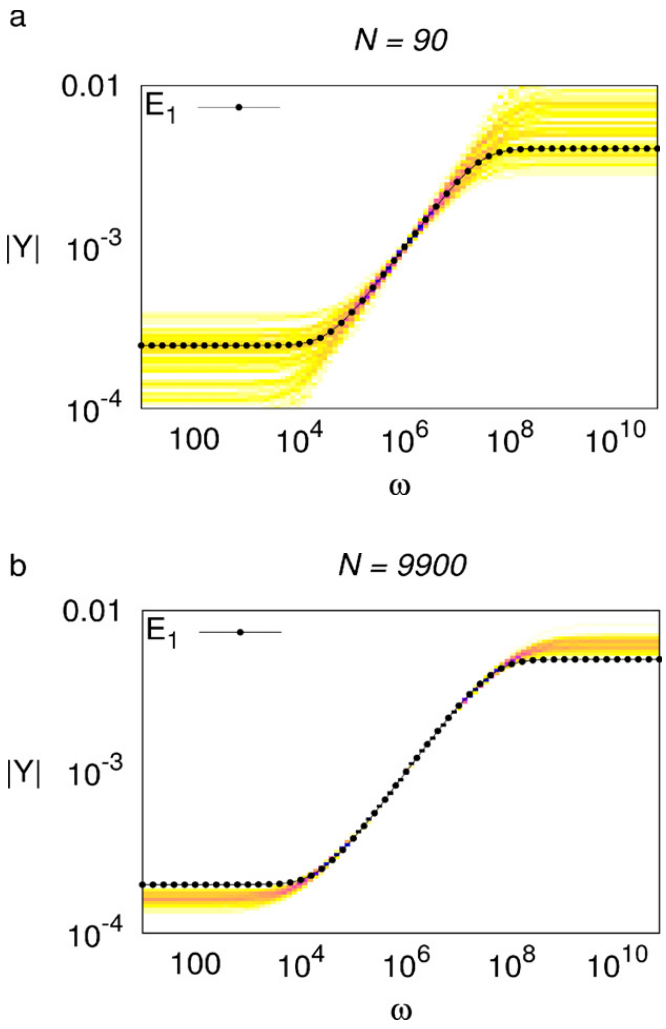

Fig. 13. (Color online) Comparison of the numerically obtained solutions of (59) with the numerical computations for many realisations of the C–R network, with $p = 0.4$ and network sizes $N = 90, 9900$.

7. Comparison of the asymptotic and numerical results

We now give two sets of calculations for finite networks. The first tests the validity of the spectral calculation in Section 5 for the case of $p = 1/2$. The second the validity of the amalgamated spectral and averaging based calculation in Section 6.

7.1. Spectral based calculations for $p = 1/2$

We firstly consider a C–R network with $\mu = \mathrm{i}\omega CR$. We compare the absolute values of the four asymptotic formulae (40)–(43) obtained by using the spectral method with the numerical calculations of the absolute network conductance $|Y|$ with $C = 1$ nF and $R = 1$ kΩ as a function of ω for four different configurations of the system, with different percolation paths for low and high frequencies. The results of this comparison are shown in Fig. 11 in which we plot the numerical calculations together with the asymptotic formulae for a range of values of N given by $N = S(S-1)$ with $S = 10, 20, 100$. We can see that the predictions of the asymptotic formulae (40)–(43) fit perfectly with the results of the numerical computations over all of the values of N considered. Indeed they agree both in the (square-root) power-law emergent region and in the four possible percolation regions, and clearly demonstrate the effect of the network size.

We next look at an R–R network with $y_1 = 1/R$ and $y_2 = \mu/R$, with real μ and R as above. Again we compare the predictions of the asymptotic formulae (40)–(43) with the numerical computations of $|Y|$ in this case. Again we see an excellent agreement in all cases, as shown in Fig. 12.

7.2. Combined averaging and spectral based calculations for general p

We now consider the responses for general p described by the pair of Eqs. (59) and (60). We compare these with numerical results for the C–R networks described in the previous sub-section. In each case of p we take the equation for which the corresponding solution in the percolation regime is physically correct.

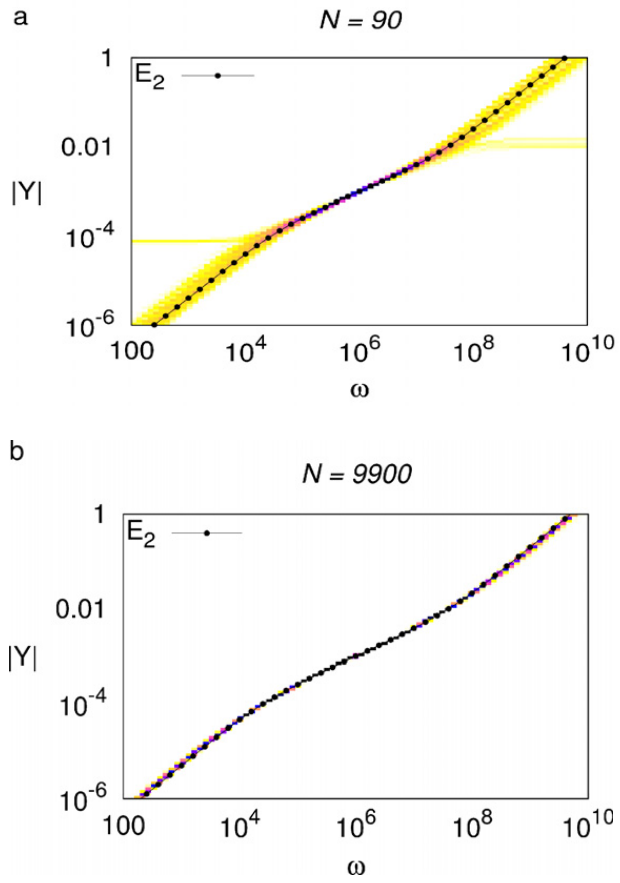

Fig. 14. (Color online) Comparison of the numerically obtained solutions of (60) with the numerical computations of $|Y(\omega)|$ for many realisations of the C–R network with $p = 0.6$ and network sizes $N = 90, 9900$.

As a first computation we take $p = 0.4$, so that $\epsilon = 0.2 > 0$, and consider a C–R network with the same values of C, R and taking $N = 90, 9900$. For an infinitely large network we expect to see resistive type percolation behaviour (with probability one) for both small and large frequencies. We compute $|Y(\omega)|$ from (59) and compare these values with the results of computations of $|Y(\omega)|$ from a large realisation of the network in Fig. 13. The results from this computation are interesting. When $N = 90$, there is quite a large statistical range in the calculations which reduces when $N = 9900$. The predictions of $|Y|$ from (59) closely follow the mid-range (PLER) of the computations for both $N = 90$ and $N = 9900$. However, as expected from the EMA results, the maximum and minimum values of $|Y|$ are slightly underestimated by (59). The results for computations of the R–R network are very similar and we do not include them here.

As a second computation we take $p = 0.6$, so that $\epsilon = -0.2 < 0$. For an infinitely large C–R network we expect to see reactive type percolation behaviour (with probability one) for both small and large frequencies. We present the results of computing $|Y(\omega)|$ from (60) compared with computations from a number of realisations of the network when $N = 90, 9900$, in Fig. 14. In this computation we again see a greater statistical range when $N = 90$ than when $N = 9900$. Indeed in the case of $N = 90$ a small number of the realisations show resistive percolation behaviour rather than reactive. This is not seen in the calculations for $N = 9900$. In both cases the results of the calculations from (60) closely match the computations over the whole range.

8. Discussion

By considering large binary networks we have shown how power-law emergence can be directly related to the statistical regularity of the spectrum of the matrices associated with the network and hence can be studied by combining spectral and averaging methods. In particular we have studied the effects of network size, and the variation from criticality on the observed power-law behaviour of these systems. We have shown how the response of the networks depends strongly upon p and less strongly on the network size N, except at $p = 1/2$ exactly, where the *dynamic range* has been found to scale in direct proportion to N. When $p = 1/2$ we analysed how the network response is described in terms of poles and zeros of the conductance and can be determined from distribution of these values, making use of numerically observed statistical patterns of these. This has revealed four asymptotic formulae, corresponding to the four qualitatively different *emergent responses* that can arise when $p = 1/2$ and these show very precisely the effects of the (finite) network size N. The case of $p = 1/2$ is very complete asymptotically and shows particularly good agreement with the numerical computations, which

is remarkable given the number of approximations made. An important open question is to now rigorously establish the observed statistical results of the spectrum in this case, for example to show rigorously that $\mu_{p,N'} \sim N$. When $p \neq 1/2$ the analysis is less complete. It is interesting, however, that the results of the averaging based EMA calculation can be combined with those of the spectral computation in a consistent manner to the case of finite N, leading to predictions (59) and (60), of the conductance and its dynamic range which is in good qualitative agreement with what is observed. However a limitation of this analysis remains the lack of precision of the estimation of the power-law scaling of the magnitude of the percolation response as $p \to 1/2$. We conclude that combining both the spectral based and the averaging based methods lead to useful asymptotic formulae with excellent numerical support, and establishing these more rigorously is an interesting area of further study.

Acknowledgements

This work was funded by the UK Engineering and Physical Sciences Research Council (EPSRC) grant number: GR/S86525/01. The authors also thank Jan Van lent for many useful discussions and insights on this problem.

References

[1] R. Bouamrane, D.P. Almond, The emergent scaling phenomenon and the dielectric properties of random resistor–capacitor networks, J. Phys. Condens. Matter 15 (24) (2003) 4089–4100.
[2] J.P. Clerc, G. Giraud, J.M. Laugier, J.M. Luck, The electrical conductivity of binary disordered systems, percolation clusters, fractals and related models, Adv. Phys. 39 (3) (1990) 191–309.
[3] B. Vainas, D.P. Almond, J. Luo, R. Stevens, An evaluation of random *R–C* networks for modelling the bulk ac electrical response of ionic conductors, Solid State Ion. 126 (1) (1999) 65–80.
[4] S. Kirkpatrick, Percolation and conduction, Rev. Mod. Phys. 45 (1973) 574–588.
[5] K.D. Murphy, G.W. Hunt, D.P. Almond, Evidence of emergent scaling in mechanical systems, Phil. Mag. 86 (21) (2006) 3325–3338.
[6] J.C. Dyre, T.B. Schrøder, Universality of ac conduction in disordered solids, Rev. Modern Phys. 72 (3) (2000) 873–892.
[7] M. Jurgawczynski, Predicting absolute and relative permeabilities of carbonate rocks using image analysis and effective medium theory, Ph.D. Thesis, University of London, 2007.
[8] G.R. Grimmett, Percolation, Springer Verlag, 1999.
[9] T. Jonckheere, J.M. Luck, Dielectric resonances of binary random networks, J. Phys. A: Math. Gen. 31 (1998) 3687–3717.
[10] G.W. Milton, Bounds on the complex dielectric constant of a composite material, Appl. Phys. Lett. 37 (1980) 300.
[11] A.K. Jonscher, Universal Relaxation Law: A Sequel to Dielectric Relaxation in Solids, Chelsea Dielectrics Press, 1996.
[12] C. Brosseau, Modelling and simulation of dielectric heterostructures: a physical survey from an historical perspective, J. Phys. D: Appl. Phys. 39 (2005) 1277–1294.
[13] K.L. Ngai, C.T. White, A.K. Jonscher, On the origin of the universal dielectric response in condensed matter, Nature 277 (5693) (1979) 185–189.
[14] A.K. Jonscher, The universal dielectric response, Nature 267 (23) (1977) 673–679.
[15] V.-T. Truong, J.G. Ternan, Complex conductivity of a conducting polymer composite at microwave frequencies, Polymer 36 (5) (1995) 905–909.
[16] D.P. Almond, B. Vainas, The dielectric properties of random *RC* networks as an explanation of the 'universal' power law dielectric response of solids, J. Phys.: Condens. Matter 11 (1999) 9081.
[17] D.P. Almond, C.R. Bowen, D.A.S. Rees, Composite dielectrics and conductors: simulation, characterization and design, J. Phys. D: Appl. Phys. 39 (2006) 1295–1304.
[18] S.R. Broadbent, J.M. Hammersley, Percolation processes, I, II, Proc. Cambridge Philos. Soc. 53 (1953) 629–641.